Non-abelian quantum Hall states and fractional charges in one dimension

Emma Wikberg

Department of Physics

Stockholm University

Thesis for the degree of Doctor of Philosophy in Theoretical Physics
Department of Physics
Stockholm University
Sweden

ISBN 978-91-7447-714-6

Printed by Universitetsservice US AB, Stockholm

Cover illustration: *What does a quasiparticle look like?* Clay figurine *Gulb* by Anders Wikberg, photo by Johan Hultgren.

Abstract

The fractional quantum Hall effect has, since its discovery around 30 years ago, been a vivid field of research—both experimentally and theoretically. In this thesis we investigate certain non-abelian quantum Hall states by mapping the two-dimensional system onto a thin torus, where the problem becomes effectively one-dimensional and hopping is suppressed, meaning that the classical electrostatic interaction dominates. The approach assists with a simplified view of ground states and their degeneracies, as well as of the nature of the fractionally charged, minimal excitations of the corresponding quantum Hall states. Similar models are also relevant for cold atoms trapped in one-dimensional optical lattices, where interaction parameters are available for tuning, which opens up for realizing interesting lattice states in controllable environments. The diverse applicability of the one-dimensional electrostatic lattice hamiltonian motivates the exploration of the systems and models treated in this work.

In the absence of hopping or tunneling, the low-energy behavior of the one-dimensional lattice system is ultimately dependent on the nature of the electrostatic interaction present. For ordinary interactions such as Coulomb, the ground state at particle filling fraction $\nu = p/q$ has a well-known q-fold center-of-mass degeneracy and the elementary excitations are domain walls of fractional charge $e^* = \pm e/q$. These appear in abelian quantum Hall systems and are known since earlier. In this work, we show how other types of interactions give rise to increased ground state degeneracies and, as a result, to the emergence of split fractional charges recognized from non-abelian quantum Hall systems.

Contents

Accompanying papers and author's contributions

Paper I **Pfaffian quantum Hall state made simple: multiple vacua and domain walls on a thin torus**
E.J. Bergholtz, J. Kailasvuori, E. Wikberg, T.H. Hansson, and A. Karlhede
Phys. Rev. B **74** 081308(R) (2006), [arXiv:cond-mat/0604251]

This paper was the basis for my diploma work and my main contribution was to use an existing computer program for exact diagonalization to construct the phase diagram in Fig. 3.3. I participated in proofreading the text but otherwise I did not take part in writing the paper.

Paper II **Degeneracy of non-abelian quantum Hall states on the torus: domain walls and conformal field theory**
E. Ardonne, E.J. Bergholtz, J. Kailasvuori, and E. Wikberg
J. Stat. Mech. (2008) P04016, [arXiv:0802.0675]

In the work which led to Paper II, I took part in figuring out the composition of the fractionally charged domain walls of the Read-Rezayi states in the thin-torus limit. I also suggested the generalization of the Su-Schrieffer argument, which is presented in the paper, and participated in writing the article. I was not involved in the CFT analysis.

Paper III **Spin chain description of rotating bosons at $\nu = 1$**
E. Wikberg, E.J. Bergholtz, and A. Karlhede
J. Stat. Mech. (2009) P07038, [arXiv:0903.4093]

For Paper III I developed a computer program for exact diagonalization from scratch and used it to extract the numerical data. I did a major part of deriving the effective spin hamiltonian for bosons at $\nu = 1$ as well as of writing the paper.

Paper IV **Fractional domain walls from on-site softening in dipolar bosons**
E. Wikberg, J. Larson, E.J. Bergholtz, and A. Karlhede
Phys. Rev. A **85** 033607 (2012), [arXiv:1109.3384]

For this paper, my contributions were to figure out the staircase phase diagram that emerges at zero tunneling and to perform the perturbative calculations. I wrote a substantial part of the paper but was not involved in the numerical analysis based on the Gutzwiller ansatz.

Paper V **Nontrivial ground-state degeneracies and generalized fractional excitations in the 1D lattice**
E. Wikberg
[arXiv:1210.7162]

Paper V is a result of my own calculations and writing.

Additional comment:
Chapters 1-5 in this thesis are modified versions of the corresponding sections in *Non-abelian Quantum Hall states on the Thin Torus*, Licentiate thesis, E. Wikberg (2009).

We lay there and looked up at the night sky and
she told me about stars called blue squares and red swirls
and I told her I'd never heard of them.

Of course not, she said, the really important stuff they never tell you.
You have to imagine it on your own.

[Brian Andreas]

Preface

The purpose of this thesis is to summarize what I have been doing for a number of years in the research group for the Theory of Quantum Matter at Stockholm University. Well aware that most doctoral theses are read by only a handful of people, my ambition has still been to make the content as accessible as possible to a somewhat broader audience (say, the general condensed matter graduate student). The advantage and beauty of the ideas and models treated in this work are their simplicity and the fact that interesting things can be understood using a minimum of mathematics. Most of the things I have done have felt as related to sudoku as to quantum physics, so if you are into both of these subjects, you might enjoy reading this.

Acknowledgements

During my time as a graduate student I have had the pleasure to get to know and work with a number of talented people, some of which have also become my close friends. I am privileged to have been surrounded by so many smart, funny and sympathetic colleagues and the best thing about writing this thesis is the opportunity to say thank you.

My supervisor Anders Karlhede has been a constant source of ideas, encouragement, knowledge and—patience. Every time I have stepped into his office to beg for more hours of teaching, he has stoically (and somewhat amused?) accepted. Also, he has devoted much of his time to reading and giving wise feedback on my work, even when he has been busy with his duties at the university management. Anders is an excellent supervisor, as well as a very kind and generous person.

The person I have been in closest collaboration with is Emil Johansson Bergholtz, now working in Berlin. During our work I have often envied his intuition for physics, as well as his extraordinary memory for details. Since I can barely remember what happened yesterday, it has been very handy to

have a living notebook and encyclopedia around. Emil is also a very good friend of mine and his support has meant a lot to me.

Eddy Ardonne, Hans Hansson, Janik Kailasvuori and Jonas Larson are co-authors of the appended papers and deserve a special mentioning for contributing with their knowledge, personal qualities and hard work in the projects. Obviously, they have been of great importance for this thesis—not least thanks to all useful discussions.

The nicest pictures contained in this thesis are drawn by Sören Holst, who has also been a much appreciated mentor during my PhD studies. My two little wizards, Mikael Fremling and Thomas Kvorning, have been of immense help by solving various layout and other computer issues. Anders, Emil and Hans have taken the time to proofread and comment on the thesis, an effort which has lead to many improvements. For the misprints, errors or craziness that might remain, I am myself fully responsible.

The physics department has not only been a place to work but also a place to see friends. Whoever thought that physicists are boring loners (Johan?) should visit our corridor. Emma, Micke, Sören and Thomas, I love our afternoon chats—you are all very dear to me. Jonas, you are the most humble assistant professor I know; if the research community were more like you, it would be a better community. Fawad H, Magnus A, Michael G, Tor K, Åsa E and other colleagues (no one forgotten!), formerly or presently at Fysikum, thank you for contributing to the friendly and open atmosphere!

Though not of any direct use when it comes to solving physics problems, my family and friends from the world outside can nevertheless take a huge amount of credit for the existence of this thesis, and some of them have been particularly exposed to my need to dwell on real or imagined worries. Christian G, thank you for pointing out that "obvious" is a dangerous word. Maria K and Maria M, thank you for reminding me that there is a world (of zombies) on the other side.

My parents Anita and Tomas, my brother Anders, and my partner in love and municipal water connection, Johan, have been of immense importance to me. Mamma och pappa, it is impossible to overrate the time, effort and commitment you put into supporting us in different ways. To buy a house at this busy stage in life was not an example of perfect timing, but I am glad we did and your help has been truly indispensable. Johan, thank you for making me laugh, for being proud of me no matter what, and for giving me something to look forward to. Lillebror, I am very proud of you (and your crazy projects!)—if I can do it, so can you.

Mormor, jag tror att jag talar för många i forskargruppen när jag säger tack för alla goda bullar.

Sammanfattning på svenska

Sedan den fraktionella kvanthalleffekten upptäcktes för omkring 30 år sedan har den varit ämne för ett aktivt och levande forskningsområde inom både experimentell och teoretisk fysik. I denna avhandling studeras ett antal icke-abelska kvanthalltillstånd genom att det tvådimensionella systemet avbildas på en tunn torus, där problemet blir effektivt endimensionellt och den elektrostatiska växelverkan dominerar över hopptermerna. Metoden bidrar med en förenklad bild av grundtillstånd och deras degeneration, såväl som av de fraktionellt laddade, minimala excitationer som tillhör motsvarade kvanthalltillstånd. Liknande endimensionella modeller är även relevanta för kalla atomer i optiska gitter, i vilka växelverkansparametrarna är tillgängliga för finjustering. Detta öppnar för möjligheten att undersöka intressanta gittertillstånd experimentellt under kontrollerbara omständigheter och den breda tillämpbarheten av den endimensionella elektrostatiska gitterhamiltonianen motiverar de undersökningar som återges i detta arbete.

I frånvaron av hopp eller tunnling är lågenergibeteendet hos partiklarna i det endimensionella gittret uteslutande beroende av den elektrostatiska växelverkan. Coulomb och andra vanliga växelverkningar är väl studerade sedan tidigare; grundtillstånden vid fyllnad $\nu = p/q$ är q-faldigt degenererade och relaterade via trivial translation av masscentrum. De elementära excitationerna, kända från abelska kvanthalltillstånd, är domänväggar mellan olika grundtillstånd och har fraktionell laddning $e^* = \pm e/q$. I detta arbete visar vi hur andra typer av växelverkningar ger upphov till utökade grundtillståndsdegenerationer mellan tillstånd som *inte* är relaterade via translation. Vi påvisar även hur en delning av de ursprungliga fraktionella laddningarna uppstår som en konsekvens av den utökade degenerationen. Resultaten är av relevans för icke-abelska kvanthallsystem, där nämnda tillstånd och excitationer återfinns.

Part I:
Background material and results

Chapter 1

The quantum Hall effect

The assemblage of systems treated in this thesis all have relevance for the quantum Hall effect, which, since it was discovered in the beginning of the 1980's, has been a source for a vast amount of condensed matter research. In this chapter we review briefly what the quantum Hall effect is, and some of the basic underlying theory. We start with a reminder of the classical Hall effect, whereafter we turn to the quantum version, introducing central concepts like fractional charge and non-abelian statistics.

1.1 The classical Hall effect

The Hall effect arises when a conducting plate is placed in a magnetic field $\mathbf{B}$, perpendicular to the surface, and a current $\mathbf{I}$ is driven through the plate (see Fig. 1.1). In 1879, the American physicist Edwin Hall discovered that under these circumstances, a non-zero voltage emerges across the plate [1]. Furthermore, the corresponding so-called Hall resistance, $R_{xy} = V_y/I$, is proportional to the magnetic field strength B, a phenomenon which is called the classical Hall effect. At the time of Hall's original experiment, the electron as a particle was yet to be discovered, but nowadays the classical Hall effect is easily explained using ordinary electromagnetism.

Each electron is affected by the Lorentz force $\mathbf{F} = e\mathbf{v} \times \mathbf{B}$, where the charge $e = -|e|$.[1] Since the velocity $\mathbf{v}$ is antiparallel to the current, the electrons will experience a force pointing in the negative y-direction, with the coordinate axes chosen as in Fig. 1.1. As the charged particles accumulate at one side of the metal plate, a potential difference builds up. In

[1] Throughout this thesis, e will denote the charge of the particles involved, even in cases where those are not electrons.

equilibrium, the magnetic force balances the electric repulsion between the electrons and a simple calculation shows that the potential difference V_y becomes proportional to B.

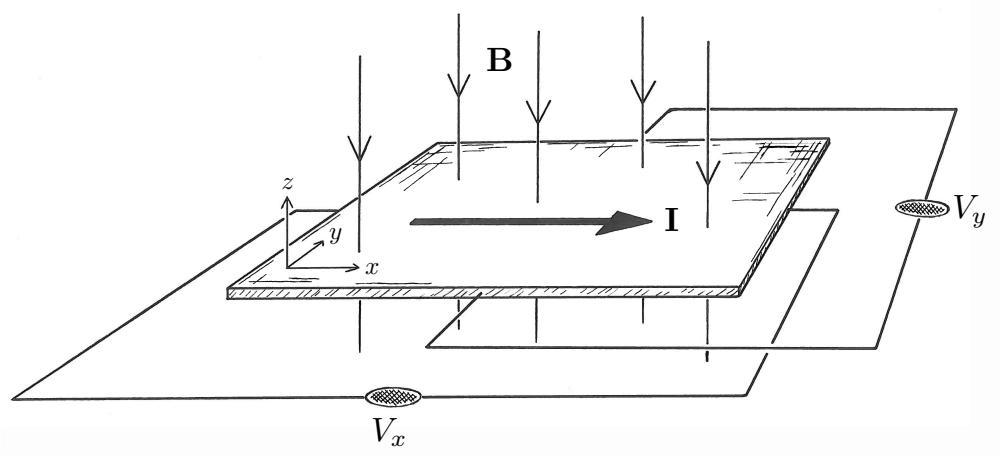

Figure 1.1: *The Hall experiment: a current* **I** *driven through a conducting plate, pierced by a transverse magnetic field* **B**. *Figure by S. Holst.*

1.2 The quantum Hall effect

About a century after Hall's achievement, the quantum version of the Hall effect was discovered in interfaces between semiconductors [2, 3], where the electrons form a two-dimensional electron gas (i.e., they are in practice unable to move in the z-direction). In very clean samples, for very low temperatures and strong magnetic fields, the previously linear dependence on B is destroyed.[2] Instead, a quantization of the Hall resistance emerges; as the magnetic field strength varies, $R_{xy} = V_y/I$ jumps between plateaus of specific values, namely

$$R_{xy} = \frac{R_K}{\nu}, \tag{1.1}$$

where $R_K = h/e^2$ is the so-called von Klitzing constant and ν takes rational values. Every integer value ν is accompanied by a plateau, while only some fractional numbers $\nu = \frac{p}{q}$ (typically with odd denominators q) give rise to the same effect, as seen in Fig. 1.2. The first case is for natural reasons

[2]The quantum Hall effect has also been realized at room temperature i graphene, see [4].

named the integer quantum Hall effect (IQHE) and it was discovered in 1980 by Klaus von Klitzing and co-workers [2]. The latter phenomenon is called the fractional quantum Hall effect (FQHE) and was first observed by Tsui, Störmer and Gossard in 1982 at $\nu = 1/3$ [3].

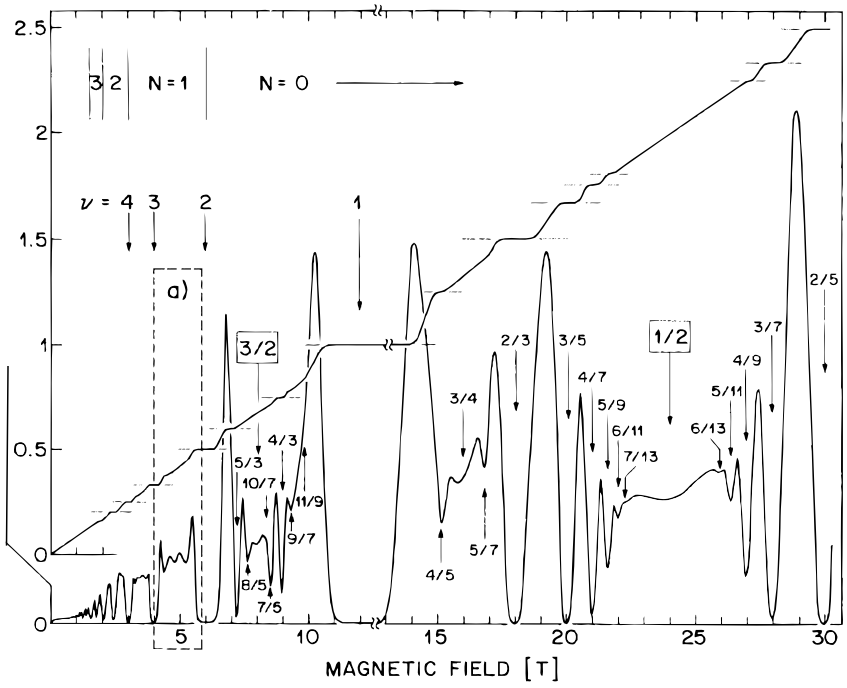

Figure 1.2: *Graph showing how the resistances R_{xy} (nearly straight line with plateaus) and R_{xx} (roller coaster curve) vary as functions of the magnetic field. Figure from Willett et al. [5].*

The reason for distinguishing the integer quantum Hall effect from the fractional quantum Hall effect is that they, despite their apparent similarity, show different behavior and require different explanations. The FQHE was the latest discovered of the two because, to make it visible, the samples need to be cleaner than required to produce the IQHE. While the integer effect is explained by solving the Schrödinger equation for a single electron in a magnetic field (see Section 2.1), the fractional ditto is an intricate consequence of strong electron-electron interactions, which makes it a more involved problem by far. A major part of this thesis is dedicated to shining light on some aspects of certain interesting FQH systems.

1.3 Basic theory

In this section we present some basic knowledge related to the quantum Hall effect. The text is by no means intended to give a complete account for the underlying theory, but merely to serve as an introduction to important concepts that will recur throughout the thesis.[3]

1.3.1 The integer effect

The IQHE can be understood by investigating the quantum mechanical properties of a single electron in a magnetic field. It turns out that the kinetic energy levels of such an electron are those of a harmonic oscillator, i.e.,

$$E_n = (n + 1/2)\hbar\omega_c, \qquad n = 0, 1, \ldots, \tag{1.2}$$

where $\omega_c \equiv \frac{|e|B}{mc}$ is the cyclotron frequency. These energy levels are called Landau levels, after the Russian physicist L.D. Landau (1908-1968), who was the first to solve this problem [7]. Each Landau level has a degeneracy that depends on the strength of the magnetic field. The number of states N_S within each energy level is

$$N_S = \frac{BA}{\Phi_0}, \tag{1.3}$$

where A is the area of the Hall plate and Φ_0 is the magnetic flux quantum, $\Phi_0 = \frac{hc}{|e|}$. In other words, N_S is given by the number of flux quanta penetrating the system.

We may now define an important quantity, namely the filling fraction ν:

$$\nu = \frac{N_e}{N_S} = \frac{N_e\Phi_0}{BA}, \tag{1.4}$$

where N_e is the number of electrons in the sample. In the low-temperature limit, the electrons in the two-dimensional electron gas will occupy the available single-particle states of lowest kinetic energy, since this energy is proportional to B, which is large. In other words, ν will be the number of filled Landau levels. The choice of label is no coincidence; the ν that appears in Eq. (1.1) is closely related to the filling fraction. The plateau with $R_{xy} = \frac{R_K}{\nu}$ is namely centered around the value $B = \frac{N_e\Phi_0}{\nu A}$, and we can now comment on the emergence of the IQHE. When ν is an integer, the ν lowest lying Landau levels will be completely filled and there is an energy gap $\hbar\omega_c$

[3] For an extended review on the quantum Hall effect, see, e.g., [6].

to the next level. In presence of disorder in the system, this energy gap will lead to a plateau in the resistance; changing the magnetic field around these points will keep R_{xy} constant.

1.3.2 The fractional effect

In general, the requirement for the quantum Hall effect to appear, besides low temperature, high magnetic field, and low amount of disorder, is the presence of a finite energy gap. The difficulty in explaining the fractional quantum Hall effect lies in the fact that, for fractional fillings, there are many ways of arranging the electrons within the highest occupied Landau level. In the absence of inter-particle interactions, this would lead to a macroscopic number of degenerate many-particle states and a gap to the next Landau level, as for the integer effect. However, the interaction lifts this degeneracy and the physics is completely determined by the filling and the nature of the interaction, as excitations within the highest occupied Landau level are possible. For some filling fractions there is a gap, whereas some fillings have a continuous energy spectrum. Indeed, for $\nu = 1/2$ and some other fractions, the resistance is *not* quantized (i.e., there is no gap), but there are many examples of fractional fillings which display plateaus in the resistance curve, as seen in Fig. 1.2. Clearly, the interaction between the electrons, which could be neglected when considering the IQHE, plays a crucial role in the FQHE and, for some filling fractions, renders a gap that gives rise to a quantization of R_{xy}. Consequently, it is a great challenge to understand the physics at various fractional fillings ν. Among the important theoretical advances, Laughlin's many-particle wave function for $\nu = \frac{1}{2m+1}$, m integer, deserves a special mentioning [8]. This trial wave function predicted and explained the emergence of the quantum Hall effect at these odd-denominator fillings, as well as their fractionally charged excitations, and gave Laughlin the Nobel Prize in 1998. Laughlin's construction has later been generalized to all fillings p/q, q odd, in a hierarchy picture of the quantum Hall system [9, 10], where higher-order QH states are constructed as condensates of quasiparticles at lower-order fillings.

1.3.3 Fractional charges and statistics

The FQHE is a topic that includes several unusual phenomena. One of those is the appearance of fractional charges—collectively induced excitations behaving like particles with fractions of an electron charge. These quasiparticles or quasiholes work as charge carriers in the quantum Hall

system at, e.g., $\nu = 1/3$, where they carry charge $e^* = \pm e/3$.[4] The size of the charge is determined by the filling fraction; $\nu = p/q$ gives fractional charge $e^* = \pm e/q$.

It should be stressed that the quasiparticles mentioned here are real fractional charges in the sense that their charge distributions are sharp. An electron whose wave function is symmetrically divided between two quantum wells yields an expectation value of $\langle Q \rangle = e/2$ for the charge in one well. However, the variance is large, so $\langle Q \rangle$ will not be interpreted as the charge of a particle. Contrarily, when measuring the charge $e^* = \pm e/q$ of the quasiparticles in the QH system, the variance can be made arbitrarily small.

Beyond the peculiar property of having a charge smaller than the particles that constitute the actual physical system, the fractional excitations obey fractional, or anyonic, statistics. This implies that the phase factor induced by an exchange of two particles is not restricted to ± 1, but may take other values $e^{i\phi}$ [13]. Some FQH excitations are also believed to obey non-abelian statistics, which similarly means that an exchange of two particles returns an entirely new state. These special features become possible as a direct consequence of the dimensionality of the system; anyons (as the particles are called) and the non-abelian dittos do not exist in three dimensions, as can be seen by the following argument.

Let us consider two indistinguishable particles and the process where one of the particles encircles the other and then returns to its initial position. We require the operation to be adiabatic, i.e., we assume finite gaps between the energy levels and move the particle so slowly that there is no energy transferred to the system. Hence, if the particles initially are in their ground state, the adiabatic process assures that the system is not excited to some higher energy level during the operation.

In three dimensions, there is no unambiguous definition of encircling a specific point in space and the path can just as well be contracted into a point. In other words, in three dimensions this operation must leave the two-particle state unaltered. Furthermore, letting one particle encircle the other is equivalent to letting them switch positions twice. Clearly, simply interchanging the particles corresponds to half of the encircling and should thus return the initial state with a factor of either plus or minus one in front, to make sure the original state is recovered if the interchange is repeated. The two alternatives are called bosonic and fermionic statistics and define the corresponding particle types bosons and fermions.

Now, consider the same operation but in two dimensions instead. In

[4] The first experimental evidence for this is presented in [11, 12].

this case there is really a way of defining what it means to go around a specific point in space. We may not shrink the path to a point and the encircling does not necessarily leave everything unchanged. Clearly, if there is no degeneracy of the ground state, we must return to the same *physical* state after the operation if adiabaticity is assumed. There is, however, a possibility for the original state to be multiplied by a phase factor. Half of the operation, i.e., interchanging the two particles, then also yields a phase factor $e^{i\phi}$. This kind of statistics is called fractional, or anyonic, statistics [13] and the corresponding particles are called anyons.

Non-abelian statistics is a generalization of fractional statistics and means that interchanging two particles (also called braiding) yields an entirely new state. This phenomenon may appear when there is a degeneracy of the states involved [14]. Since there is no energy transfer needed to put the system in the degenerate state, the adiabaticity does not prevent the particles from switching to one of those states in the process.

In the quantum Hall effect, non-abelian statistics appears as a consequence of an *increased* degeneracy of the ground state (we will expand on this later on) [14]. Because of the nontrivial degeneracy, the ordinary fractional charges $e^* = \pm e/q$ in those systems are split; the non-abelian system at $\nu = 5/2$ displays charge carriers $e^* = \pm e/4$. Due to the differences between "ordinary" quantum Hall states and the *non-abelian* dittos, the first will be denoted *abelian* quantum Hall states, and their quasiparticles abelian anyons.[5]

[5]For a nice viewpoint paper on non-abelian anyons, see [15].

Chapter 2

One-dimensional picture of the quantum Hall system

The fractional quantum Hall system is an intriguing example of strongly correlated electrons in two dimensions. In general, this many-body problem is impossible to solve exactly. However, the basis for the work contained in this thesis is the lucky discovery that in a certain geometry and a certain mathematical limit, the unsolvable two-dimensional problem turns into a solvable one-dimensional problem. This chapter is dedicated to presenting the connection between the experimental two-dimensional quantum Hall system and a one-dimensional lattice system.

Our starting point will be to solve the quantum mechanical problem of a single electron in a magnetic field on a torus. This results in a mapping of the two-dimensional QH system onto a one-dimensional lattice. Furthermore, letting the circumference of the torus go to zero reduces the involved quantum mechanical many-body problem to simple electrostatics. A brief review of the earliest studies that made use of this mathematical trick shows that many features of the bulk system remain in the thin-torus limit and motivates continued investigations using this approach.

2.1 Electron in a magnetic field

Let us calculate the energy eigenstates for an electron in two dimensions in the presence of a magnetic field, perpendicular to the plane of motion. We do this using the geometry of a cylinder (periodic boundary conditions in one direction) and then generalize our results to a torus (periodic boundary conditions in both directions).

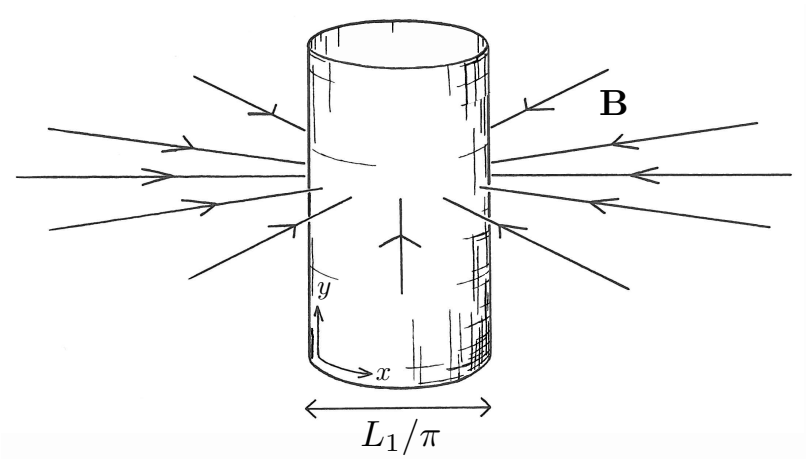

Figure 2.1: *A cylinder with circumference L_1, pierced by a magnetic field* **B**. *Figure by S. Holst.*

Consider the situation in Fig. 2.1, where L_1 is the circumference of the cylinder. The so-called Landau gauge, $\mathbf{A} = By\hat{x}$, gives a magnetic field pointing in the negative z-direction since $\mathbf{B} = \nabla \times \mathbf{A} = -B\hat{z}$. To enter the magnetic field into the Schrödinger equation, we start with the hamiltonian of a free particle in two dimensions and modify this by minimal coupling:

$$\mathbf{p} \to \mathbf{p} - \frac{e}{c}\mathbf{A}, \tag{2.1}$$

which yields

$$\hat{H} = \frac{1}{2m}\Big(\Big(\hat{p}_x + \frac{|e|B}{c}y\Big)^2 + \hat{p}_y^2\Big). \tag{2.2}$$

The question is: What are the energy eigenfunctions of this hamiltonian?

A good choice of separating ansatz is

$$\psi_k(x, y) = e^{ikx}\phi(y), \tag{2.3}$$

which together with periodic boundary conditions in the x-direction,

$$\psi_k(x, y) = \psi_k(x + L_1, y), \tag{2.4}$$

implies

$$k = \frac{2\pi q}{L_1}, \qquad q = 0, \pm 1, \ldots. \tag{2.5}$$

The wave function (2.3) is clearly an eigenstate of $\hat{p}_x$ with eigenvalue $\hbar k$. This means that we are allowed to replace the $\hat{p}_x$ operator by $\hbar k$ in the hamiltonian, and the x-dependence is eliminated. We can then divide both sides in the Schrödinger equation by e^{ikx} and we are left with

$$\hat{H}_k \phi(y) = E_k \phi(y), \tag{2.6}$$

where

$$\hat{H}_k \equiv \frac{1}{2m}\Big(\hat{p}_y^2 + \Big(\hbar k + \frac{|e|B}{c} y\Big)^2\Big). \tag{2.7}$$

We recognize this as the hamiltonian of a one-dimensional harmonic oscillator and can immediately write down the energy eigenvalues

$$E_{nk} = (n + 1/2)\hbar\omega_c, \qquad n = 0, 1, \ldots, \tag{2.8}$$

where $\omega_c \equiv \frac{|e|B}{mc}$ is the cyclotron frequency. As mentioned in Chapter 1, these energy levels are called Landau levels [7]. Note also that, according to Eq. (2.7), the wave functions are centered around $y = -k\ell^2$, where $\ell \equiv \sqrt{\frac{\hbar c}{|e|B}}$ is the so-called magnetic length. With this definition, the energy eigenfunctions become

$$\psi_{nk}(x, y) = \frac{1}{\sqrt{\pi^{1/2} 2^n n! L_1}} e^{ikx} H_n(y + k\ell^2) e^{-\frac{1}{2\ell^2}(y+k\ell^2)^2}, \tag{2.9}$$

where H_n are the Hermite polynomials $H_0 = 1$, $H_1(\xi) = 2\xi$, $H_2(\xi) = 4\xi^2 - 2$, etc..

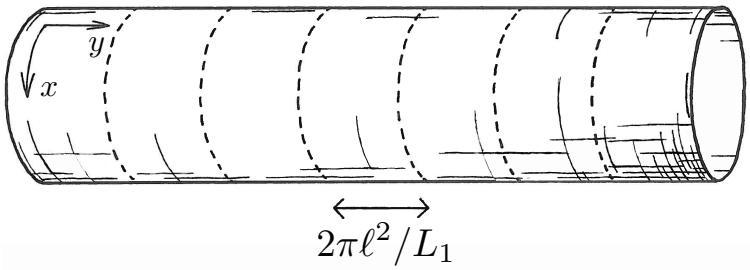

Figure 2.2: *Illustration of how the single-particle states are centered along the dotted lines at $y = -k\ell^2$. The distance between two neighboring states is $2\pi\ell^2/L_1$. Figure by S. Holst.*

Since consecutive k-values differ by $\frac{2\pi}{L_1}$, the distance between the centers of the associated wave functions is $\frac{2\pi\ell^2}{L_1}$, as illustrated in Fig. 2.2. In the following section this will be used to construct a lattice model for the quantum Hall system, but let us first identify the filling fraction ν.

The area per state in a Landau level is $2\pi\ell^2$ (see Fig. 2.2), so the density of states is $n_s = 1/2\pi\ell^2$. If we let n_e be the electron density, the number of filled Landau levels is

$$\nu = \frac{n_e}{n_s} = 2\pi\ell^2 n_e = \frac{hcn_e}{|e|B} = \frac{n_e\Phi_0}{B}, \tag{2.10}$$

which agrees with Eq. (1.4). Through the rest of this thesis we impose $\ell = 1$, i.e. the area per state is 2π. With L_2 being the length (in the y-direction) of the cylinder, this leads to the relation $L_1L_2 = 2\pi N_s$, where N_s is the number of states in a Landau level.

2.2 One-dimensional lattice model

Let us turn to consider the full quantum Hall problem—the interacting many-particle system. We restrict our studies to a single Landau level, motivated by the assumption that the magnetic field is so large that the electrons will fill the lowest Landau levels before minimizing their mutual interaction energy, and that the completely filled Landau levels are inert. (This will be fulfilled exactly in the limit $B \to \infty$, where the gap between the Landau levels grows large.) In effect then, the kinetic energy of the electrons is a constant that can be subtracted from the hamiltonian, which consequently consists of the inter-particle potential energy only.[1] Finally, we assume that we have complete spin-polarization, also due to the large magnetic field. Clearly, since the electrons are spin-1/2 particles, there is room for $2N_s$ particles in each Landau level. In other words, filling $\nu = 2$, e.g., means that the lowest Landau level is completely filled with both spin-ups and spin-downs.

2.2.1 Fock-space representation

With these assumptions we may consider many-particle states where each single-particle state $\psi_{nk}(x, y) \equiv \psi_k(x, y)$ is either occupied by an electron or empty. The single-particle states are centered along lines (see Fig. 2.2) that can be pictured as sites in a one-dimensional lattice. Hence, we can perform

[1] Interaction with the disorder in the system is ignored.

a mapping onto a series of zeros and ones ("Fock-space representation"), where a one at the kth position denotes an electron in the state centered at $y = -k$ in units of the lattice spacing $2\pi/L_1$ (see Fig. 2.3).[2] In other words, a one at this position corresponds to an electron with x-momentum $-\frac{2\pi}{L_1}k$. The correspondence between the many-particle lattice states and the single-particle real-space states is, since we are dealing with fermions, a Slater determinant:

$$|n_0\ n_1 \ldots n_{N_s-1}\rangle \doteq \frac{1}{\sqrt{N_e!}} \begin{vmatrix} \psi_{k_1}(\mathbf{r}_1) & \psi_{k_1}(\mathbf{r}_2) & \ldots & \psi_{k_1}(\mathbf{r}_{N_e}) \\ \psi_{k_2}(\mathbf{r}_1) & \psi_{k_2}(\mathbf{r}_2) & \ldots & \psi_{k_2}(\mathbf{r}_{N_e}) \\ \vdots & \vdots & \ddots & \vdots \\ \psi_{k_{N_e}}(\mathbf{r}_1) & \psi_{k_{N_e}}(\mathbf{r}_2) & \ldots & \psi_{k_{N_e}}(\mathbf{r}_{N_e}) \end{vmatrix}, \quad (2.11)$$

where $n_i = 0,\ 1$ and $\sum_{i=0}^{N_s-1} n_i = N_e$.[3] (Like before, N_s is the number of electron states in a Landau level.) A general many-particle state with N_e electrons is a linear combination of these states.

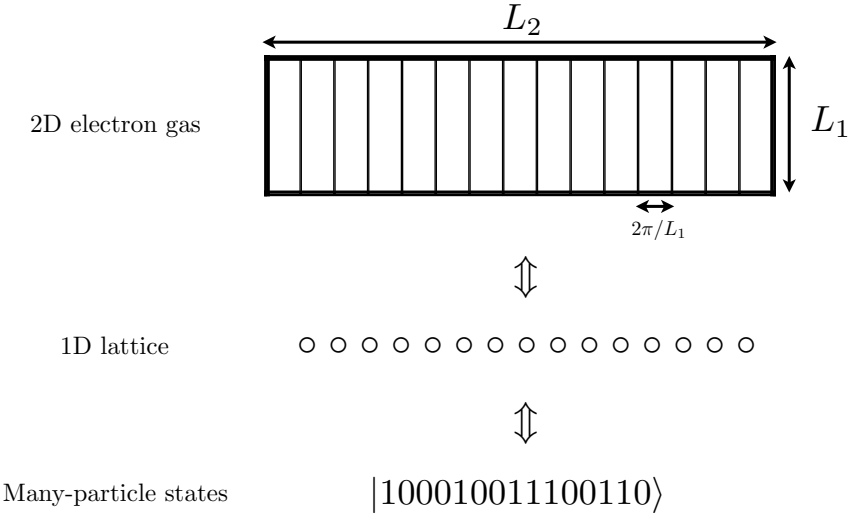

Figure 2.3: *Mapping of the two-dimensional electron gas onto a one-dimensional lattice, the many-particle states being binary strings.*

[2]The first lattice site to the left here corresponds to $k = 0$.

[3]Here, $\doteq$ means that the state is *represented* by the wave function in position space of the particles, i.e., $|n\rangle \doteq \psi(\mathbf{r})$ means $\langle \mathbf{r}|n\rangle = \psi(\mathbf{r})$, etc..

2.2.2 Translation operators and symmetries

Following Haldane [16], we will now introduce two translation operators, $\hat{T}_1$ and $\hat{T}_2$, which act on the many-particle lattice states. Consider a torus, i.e., our cylinder but with the ends connected so that the first and last sites are separated by one lattice constant—in other words, we require periodic boundary conditions also in the y-direction. We define $\hat{T}_2$ to be an operator that translates the entire lattice configuration one step to the right (i.e., in the positive y-direction);

$$\hat{T}_2|n_0\ n_1 \dots n_{N_s-1}\rangle = |n_{N_s-1}\ n_0 \dots n_{N_s-2}\rangle. \tag{2.12}$$

Similarly, $\hat{T}_1$ is a translation operator acting in the x-direction, with the effect that it picks out the x-momenta of the electrons, and the eigenvalues are $e^{\frac{i2\pi}{N_s}\sum_{k=0}^{N_s-1} kn_k} \equiv e^{i2\pi K/N_s}$.

The lattice states of Eq. (2.11) are eigenstates of $\hat{T}_1$;

$$\hat{T}_1|n_0\ n_1 \dots n_{N_s-1}\rangle = e^{i2\pi K/N_s}|n_0\ n_1 \dots n_{N_s-1}\rangle, \tag{2.13}$$

where

$$K = \sum_{k=0}^{N_s-1} kn_k\ mod\ N_s. \tag{2.14}$$

K is thus the sum of the momenta (in units of $2\pi/L_1$) of the particles in the lattice, taken modulo N_s. This quantum number characterizes the eigenstates of $\hat{T}_1$. For the two-particle state in the example above, $K = 0 + 3 = 3$.

Because of the translation invariance on the torus, both $\hat{T}_1$ and $\hat{T}_2$ commute with the hamiltonian, i.e., $[\hat{T}_1, \hat{H}] = [\hat{T}_2, \hat{H}] = 0$. However, $[\hat{T}_1, \hat{T}_2] \neq 0$ because $\hat{T}_2$ in general shifts the sum of the x-momenta. But let us now consider the electron gas at filling $\nu = p/q = N_e/N_s \ \Leftrightarrow\ pN_s = qN_e$. What happens if we let $\hat{T}_2^q$ act on one of the lattice states (which are eigenstates of $\hat{T}_1$)? Each electron will move q steps to the right, increasing K by $N_e q$. Some of them, though, might at the same time "fall over the edge" of the lattice, appearing at the left end again, which decreases K by mN_s, where m is the number of electrons falling over the edge. In total, acting with $\hat{T}_s^q$ on an eigenstate of $\hat{T}_1$ gives a change in K that is $\Delta K = N_e q - mN_s = (p-m)N_s$. Because p and m are integers, taking $\Delta K\ mod\ N_s$ gives zero. This means that the operator $\hat{T}_2^q$ conserves the quantum number of $\hat{T}_1$ and hence that $[\hat{T}_2^q, \hat{T}_1] = 0$. Since $[\hat{T}_2, \hat{H}] = 0$ it also follows that $[\hat{T}_2^q, \hat{H}] = 0$.

The operators $\hat{T}_1$ and $\hat{T}_2^q$ form a maximal set of commuting operators together with the hamiltonian, $\hat{H}$. The three operators are simultaneously

diagonalizable, and their common eigenstates constitute a complete set of basis states. This fact can be exploited in the process of diagonalizing the many-body hamiltonian; if the common eigenstates of $\hat{T}_1$ and $\hat{T}_2^q$ are used as the basis, the matrix representation of $\hat{H}$ will have non-zero elements only for coupling between eigenstates with the same $\hat{T}_1$ and $\hat{T}_2^q$ quantum numbers. Hence, it can be valuable to determine these eigenstates.

Acting N_s times with $\hat{T}_2$ on a state with N_s lattice sites must return the original state. Hence, $\hat{T}_2^{N_s} = 1$, and the eigenvalue of $\hat{T}_2^{N_s}$ is 1. However, we are interested in the eigenvalues of $\hat{T}_2^q$. We rewrite $1 = \hat{T}_2^{N_s} = \left(\hat{T}_2^q\right)^{N_s/q}$, which implies that the eigenvalues of $\hat{T}_2^q$ are $a_N = e^{i2\pi Nq/N_s}$, where $N = 0, 1, ..., \frac{N_s}{q} - 1$. N is thus the quantum number of $\hat{T}_2^q$.

Now, let us consider the eigenstates of $\hat{T}_2^q$. The following procedure automatically constructs such states which are also eigenstates of $\hat{T}_1$, i.e., with determined K-value. For each eigenvalue a_N, start with one of the states $|n_0\ n_1 \dots n_{N_s-1}\rangle \equiv |\tilde{\Psi}\rangle$ and form the (unnormalized) state

$$|\Psi\rangle \equiv (1 + a_N^{-1}\hat{T}_2^q + a_N^{-2}\hat{T}_2^{2q} + \dots + a_N^{-(N_s/q-1)}\hat{T}_2^{q(N_s/q-1)})|\tilde{\Psi}\rangle. \qquad (2.15)$$

One can easily show that these states are eigenstates of $\hat{T}_2^q$, i.e. $\hat{T}_2^q|\Psi\rangle = a_N|\Psi\rangle$. (For some choices of a_N and $|\tilde{\Psi}\rangle$, the expression in (2.15) will however give a trivial zero, in which case we have tried to match the eigenvalue with the wrong state.)

At this stage it is appropriate to comment on the degeneracy of the energy eigenstates. Since $\hat{H}$ and $\hat{T}_2$ commute, it follows that translating an entire lattice configuration between 1 and $q-1$ steps in the y-direction yields new states with the same energy: $\hat{H}|\Psi\rangle = E|\Psi\rangle \Rightarrow \hat{H}\hat{T}_2|\Psi\rangle = E\hat{T}_2|\Psi\rangle$, $\hat{H}\hat{T}_2^2|\Psi\rangle = E\hat{T}_2^2|\Psi\rangle$,... $\hat{H}\hat{T}_2^{q-1}|\Psi\rangle = E\hat{T}_2^{q-1}|\Psi\rangle$. (Acting once more with $\hat{T}_2$ on $|\Psi\rangle$ will return the original state, since $|\Psi\rangle$ is an eigenstate of $\hat{T}_2^q$ as well.) Note that all these translated states have different K-values, hence they are orthogonal. There is, in other words, an *at least* q-fold degeneracy of the many-particle energies at filling $\nu = p/q$.

Example

Consider $\nu = 1/2$, where each state may be labeled by the quantum numbers K and N of $\hat{T}_1$ and $\hat{T}_2^2$ respectively, and choose for simplicity $N_s = 4$. We search for the combinations of different $|n_0\ n_1\ n_2\ n_3\rangle$ that are eigenstates of $\hat{T}_1$ and $\hat{T}_2^2$.

First note that the number of ways to arrange two identical particles at four different sites is $\binom{4}{2} = 6$. We list the different possibilities and their

K-values here:

$|1100\rangle$; $K = 1\ mod\ 4 = 1$,
$|1010\rangle$; $K = 2\ mod\ 4 = 2$,
$|1001\rangle$; $K = 3\ mod\ 4 = 3$,
$|0110\rangle$; $K = 3\ mod\ 4 = 3$,
$|0101\rangle$; $K = 4\ mod\ 4 = 0$,
$|0011\rangle$; $K = 5\ mod\ 4 = 1$.

Since we search for eigenstates of $\hat{T}_1$, combining states with different K-values is not permitted. For example, the state $|1100\rangle + |1010\rangle$ is not allowed since $|1100\rangle$ has $K = 1$ and $|1010\rangle$ has $K = 2$. In the example, the second state is the only one with $K = 2$. Hence, it cannot be connected to any of the other states. We note that it is an eigenstate of $\hat{T}_2^2$ with quantum number $N = 0$, since $\hat{T}_2^2|1010\rangle = |1010\rangle = e^{i2\pi 0/2}|1010\rangle$. The similar thing holds for the fifth state, which has $K = N = 0$.

What about the four remaining states? Two by two they share the same K-value, but neither of them is alone an eigenstate of $\hat{T}_2^2$. If we do not immediately see the solution, we may use the general method described above to find the right combinations. Let us, for example, try with $a_N = a_1 = -1$ and $|\tilde{\Psi}\rangle = |1001\rangle$:

$$|\Psi\rangle = \left(1 + \frac{1}{-1}\hat{T}_2^2\right)|\tilde{\Psi}\rangle = |1001\rangle - |0110\rangle \tag{2.16}$$

so that

$$\hat{T}_2^2|\Psi\rangle = |0110\rangle - |1001\rangle = -|\Psi\rangle = a_1|\Psi\rangle. \tag{2.17}$$

Thus, $|1001\rangle - |0110\rangle$ has $(K, N) = (3, 1)$. This and the remaining results are summarized below:

$|1010\rangle : (K, N) = (2, 0)$,
$|0101\rangle : (K, N) = (0, 0)$,
$|1100\rangle + |0011\rangle : (K, N) = (1, 0)$,
$|1100\rangle - |0011\rangle : (K, N) = (1, 1)$,
$|1001\rangle + |0110\rangle : (K, N) = (3, 0)$,
$|1001\rangle - |0110\rangle : (K, N) = (3, 1)$.

For $\nu = 1/2$, the degeneracy of the energy eigenvalues is at least two, and the trivially degenerate states are related by simple center-of-mass translations one step in the y-direction. We check this by noting that, e.g., $|1010\rangle$ and $|0101\rangle$ are related by this kind of translation.

2.2.3 Field-operator hamiltonian

The one-dimensional lattice model provides a simple way to construct the hamiltonian describing the electron-electron interactions. Let us define the field operator $\hat{\Psi}^\dagger(\mathbf{r})$:

$$\hat{\Psi}^\dagger(\mathbf{r}) \equiv \sum_k \psi_k^*(\mathbf{r}) c_k^\dagger, \quad \{c_n^\dagger, c_m\} = \delta_{mn}, \tag{2.18}$$

where $c_k^\dagger$ (c_k) is an operator that creates (annihilates) an electron in the state ψ_k. The electron density is $\hat{\rho}(\mathbf{r}) = \hat{\Psi}^\dagger(\mathbf{r})\hat{\Psi}(\mathbf{r})$ and the hamiltonian for the interaction energy between the electrons is[4]

$$\begin{aligned} \hat{H} = \frac{1}{2}\int\int : \hat{\rho}(\mathbf{r}_1) V(\mathbf{r}_1 - \mathbf{r}_2)\hat{\rho}(\mathbf{r}_2) : d^2r_1 d^2r_2 = \\ = \sum_{k_1 k_2 k_3 k_4} V_{k_1 k_2 k_3 k_4} c_{k_1}^\dagger c_{k_2}^\dagger c_{k_3} c_{k_4}, \end{aligned} \tag{2.19}$$

where

$$V_{k_1 k_2 k_3 k_4} = \frac{1}{2}\int\int \psi_{k_1}^*(\mathbf{r}_1)\psi_{k_2}^*(\mathbf{r}_2) V(\mathbf{r}_1 - \mathbf{r}_2)\psi_{k_3}(\mathbf{r}_2)\psi_{k_4}(\mathbf{r}_1) d^2r_1 d^2r_2. \tag{2.20}$$

On the torus,

$$V_{k_1 k_2 k_3 k_4} = \frac{\delta'_{k_1+k_2, k_3+k_4}}{2N_s} \sum_{q_1, q_2} \delta'_{k_1 - k_4, q_1 L_1/2\pi} \tilde{V}(\mathbf{q}) e^{-\frac{q^2}{2} - i(k_1 - k_3)\frac{q_2 L_2}{N_s}}, \tag{2.21}$$

where $\tilde{V}(\mathbf{q})$ is the two-dimensional Fourier transform of $V(\mathbf{r})$ and δ' is the periodic Kronecker delta (with period N_s) [17]. The sum is over all allowed wave vectors on the torus, i.e., $q_\alpha = \frac{2\pi n_\alpha}{L_\alpha}$, $n_\alpha = 0, \pm 1, \ldots$. For Coulomb interaction, the Fourier transform of $V(\mathbf{r}) = \frac{1}{r}$ is $\tilde{V}(\mathbf{q}) = \frac{1}{q}$.

The sum in Eq. (2.19) contains both electrostatic terms and hopping terms, the latter corresponding to electrons hopping between sites in the lattice. The electrostatic terms may be divided into two cases. For $k_1 = k_4$, $k_2 = k_3$, particles 1 and 2 keep their original k-values (c.f. Eq. (2.20))—this is called *direct interaction*. Contrarily, $k_1 = k_3$, $k_2 = k_4$, which corresponds to particle 1 and 2 switching places in the lattice, is referred to as electrostatic *exchange interaction*. For hopping, none of these conditions on k_i are

[4] Compare with the classical expression $H_{cl} = \frac{1}{2}\int\int \rho(\mathbf{r}_1) V(\mathbf{r}_1 - \mathbf{r}_2)\rho(\mathbf{r}_2) d^2r_1 d^2r_2$. The symbol :: implies normal ordering, i.e., all creation operators are put to the left of the annihilation operators (this is a way of preventing the empty lattice from yielding non-zero energy terms).

fulfilled; the occupied sites shift in the process. However, the total momentum of the particles must of course be conserved. Here, this is equivalent to conserved center-of-mass position. Since the lattice sites are numbered with the single-particle momenta, $k_1 + k_2 = k_3 + k_4$ must hold, which readily eliminates one of the sums in (2.19). In the torus geometry, we have periodic boundary conditions in the y-direction as well; translating every electron the same number of lattice sites should not change the energy of the system. This leads to an extra requirement on k_i, i.e., we need only two indices on V and the hamiltonian for the torus can be written

$$\hat{H} = \sum_i \sum_{|m|<k\leq N_s/2} V_{km} c^\dagger_{i-k} c^\dagger_{i+m} c_{i-k+m} c_i =$$

$$= \sum_i \sum_{0\leq m<k\leq N_s/2} V_{km} c^\dagger_{i-k} c^\dagger_{i+m} c_{i-k+m} c_i + h.c. \equiv \sum_{0\leq m<k\leq N_s/2} \hat{V}_{km}, \quad (2.22)$$

where

$$V_{km} = \frac{1}{2^{\delta_{k,N_s/2}}} (V_{i+m,i+k,i+m+k,i} - V_{i+m,i+k,i,i+m+k} + V_{i+k,i+m,i,i+m+k} - V_{i+k,i+m,i+m+k,i}). \quad (2.23)$$

It is evident from Eq. (2.22) that V_{k0} is the electrostatic interaction energy of two electrons at the distance k from each other. V_{km} ($m \neq 0$) is the matrix element for the hopping of two electrons from a distance $k+m$ to a distance $k-m$ from each other, or vice versa, as illustrated in Fig. 2.4.

$$\underbrace{1...0...0...1}_{k+m} \quad \overset{\hat{V}_{km}}{\Longleftrightarrow} \quad 0...\underbrace{1...1}_{k-m}...0$$

Figure 2.4: *Illustration of the effect of the operator $\hat{V}_{km}$. Note that the hopping preserves the center of mass, i.e., the total momentum.*

2.3 The thin-torus limit

The idea of describing the quantum Hall system on a cylinder or a torus is purely a mathematical construction; to actually recreate this setup physically would, e.g., require the existence of magnetic monopoles. The periodic

boundary conditions are merely imposed to simplify the problem and get rid of boundary effects. However, we know that letting the torus circumferences in both the x- and the y-directions go to infinity will correspond to the experimental, infinite planar geometry. The suggestion to explore the model in an opposite limit, letting $L_1 \to 0$, thus sounds a bit strange at first. This is, however, exactly what we will do.

2.3.1 Energy eigenstates in the thin limit

Working in the thin-torus limit has the advantage of making theoretical calculations and considerations much simpler. The reason is the fact that as $L_1 \to 0$, all hopping terms in the hamiltonian vanish. It can be seen from Eq. (2.20) that hopping becomes unimportant as $L_1 \to 0$. As we already know, in this limit the lattice sites become widely separated. This means that the overlap between two wave functions centered at different lattice points tends to zero. For hopping terms, the wave functions for four different k-values are multiplied to give the matrix elements, hence those become extremely small. For the electrostatic exchange terms, the matrix elements are

$$V_{k_1k_2k_3k_4} = \frac{1}{2}\int\int \psi^*_{k_1}(\mathbf{r}_1)\psi^*_{k_2}(\mathbf{r}_2)V(\mathbf{r}_1-\mathbf{r}_2)\psi_{k_1}(\mathbf{r}_2)\psi_{k_2}(\mathbf{r}_1)d^2r_1d^2r_2. \quad (2.24)$$

We see that only two different wave functions are involved. However, $\psi^*_{k_1}$, ψ_{k_1}, and $\psi^*_{k_2}$, ψ_{k_2}, are evaluated at different points in space, and hence even these overlaps will be extremely small. In contrast, the direct terms are

$$V_{k_1k_2k_3k_4} = \frac{1}{2}\int\int \psi^*_{k_1}(\mathbf{r}_1)\psi^*_{k_2}(\mathbf{r}_2)V(\mathbf{r}_1-\mathbf{r}_2)\psi_{k_2}(\mathbf{r}_2)\psi_{k_1}(\mathbf{r}_1)d^2r_1d^2r_2, \quad (2.25)$$

in which case we get non-zero overlaps even though ψ_{k_1}, ψ_{k_2} are widely separated.

We conclude that in the thin limit, all interaction terms except for the direct electrostatic V_{k0} are suppressed. The hopping and exchange terms may be neglected and the full interacting quantum Hall system reduces to a classical one-dimensional electrostatics problem captured by

$$\hat{H} = \sum_i \sum_{0<k\leq N_s/2} V_{k0}\hat{n}_i\hat{n}_{i+k}, \quad (2.26)$$

c.f. Eq. (2.22). In effect, the energy eigenstates are just crystalline configurations where the electrons are located at specific lattice sites. More

specifically, for all ordinary interactions, like Coulomb repulsion, the ground state minimizes the electrostatic energy by spreading the electrons out as evenly as possible on the lattice. These thin-limit ground states are called Tao-Thouless (TT) states [18].

As an example, the ground state at filling $\nu = 1/q$ has one particle on every qth site. For $\nu = 1/3$ it is $|100100100...\rangle \equiv [100]$ (three center-of-mass translations), where we have introduced the unit cell within square brackets as a short-hand notation for the many-particle state. In general, at $\nu = p/q$ the ground state has p particles in every string of q consecutive sites and the q-fold degeneracy mentioned in Section 2.2.2 originates from a trivial center-of-mass translation of the ground state unit cell of length q.

2.3.2 Fractional charges in the thin limit

In Section 1.3.3 we mentioned the exotic phenomenon of fractional charges in the quantum Hall system. We will now take advantage of the crystalline-like states in the thin limit to explore how abelian fractional charges can be created in a lattice state [19,20]. By forming domain walls between different translations of the degenerate TT state at filling $\nu = 1/q$, fractional charges $e^* = \pm e/q$ are created. This procedure will be generalized in later chapters of this thesis, where also non-abelian domain wall excitations are treated.

As a concrete example, consider $\nu = 1/3$. In the thin limit the ground state is the TT state $[100] = |100100100...\rangle$. Let us consider three domain walls between this state and the translated states [001] and [010]:

$$[100][001][010][100] \equiv |...100\underline{101}00100100\underline{101}00100100\underline{101}00100...\rangle.$$

At the three domain walls there are concentrations of negative charge (red color and underlined in the sequence). But compared to the original lattice state [100], there is only *one more electron* in total in the series. Therefore, we must see the three charge densifications as sharing this extra charge e. We conclude that each domain wall corresponds to a fractional charge $e^* = e/3$. This is an illustration of the so-called Su-Schrieffer counting argument [21]. In general, a set of q domain walls in the $\nu = 1/q$ system yields q charges of size $\pm e/q$ (the sign depending on how the ground states are combined). However, the number of excitations in a state is not limited to an integer number times q; single domain walls can just as well be created.

Fractional charges appear in excited states at the exact fillings $\nu = p/q$. To maintain the filling fraction, one positive and one negative fractional charge of the same size appear at different places in the lattice. Due to the

opposite signs, the quasiparticles attract each other and the more separate they are, the larger energy the excited state has. However, when moving slightly away from the exact filling (e.g., by adding or removing an empty site from $\nu = 1/3$), the fractional charges appear in the ground state configuration.

2.3.3 Experimental relevance

By now it should be evident that putting the quantum Hall system on a thin torus is a mathematical trick that immensely simplifies the diagonalization of the many-body hamiltonian. However, it is by no means obvious that the extreme mathematical limit has any bearing on reality. Rather surprising though, it has been shown [22] that many of the physical features of the quantum Hall system survive in this limit. In fairly recent studies of the QH system on the torus, see, e.g., [22–24], the connection between the thin torus and the bulk has been explored. Good arguments have been given for that the "crystalline" ground states at abelian quantum Hall fillings evolve continuously from the thin limit to the physical bulk states as $L_1 \to \infty$. This implies that the TT ground states at these fractions, in spite of their simplicity, display the important physics of the bulk; the gap, the correct quantum numbers and the fractionally charged excitations.

For gapless fillings (e.g., $\nu = 1/2$), and non-abelian QH fillings (e.g., $\nu = 5/2$) on the other hand, there must be a phase transition between the thin limit and the bulk. All TT states are gapped, since it takes a finite electrostatic energy to rearrange the electrons to some other crystalline state, and this is not consistent with the gapless fillings. Furthermore, fractional charges do not appear in the system at non-QH fillings, like $\nu = 1/2$, where the resistance is not quantized. Non-abelian fillings require increased ground state degeneracies (on top of the q-fold center-of-mass degeneracy) and an extra splitting of the abelian charges, which generally is not seen in the thin limit.[5] These facts do not necessarily mean that the thin-torus approach is useless for gapless and non-abelian fillings; for at least some systems like these, the phase transition takes place on a very thin torus and the physics can still be understood by studying the physics on a thin, but not infinitely thin, torus. We will see examples of this in the coming chapters.

[5] The q-fold degeneracy is a trivial consequence of the chosen torus geometry—this degeneracy is not present on the plane and cannot cause non-abelian statistics.

2.4 Review of an exact solution for $\nu = 1/2$

The first indication of the usefulness of studying the quantum Hall system on the thin torus came from an analysis of the half-filled lowest Landau level, $\nu = 1/2$, which gave a microscopical explanation for the gapless nature of this system [22, 25]. The study treats $\nu = 1/2$ on a finitely thin torus, in a regime where the low-energy sector may be mapped onto a one-dimensional spin-1/2 chain and the ground state is described by an exact solution of a truncated hamiltonian. We will here review the basic and most important features of this study to later expand the analysis to fermions at filling $\nu = 5/2$ and bosons at $\nu = 1$.

Consider $\nu = 1/2$ on the torus. In the thin limit, $L_1 \to 0$, the ground state is the TT state $[10] = |101010...\rangle$ (and, of course, the trivial translation $[01] = |010101...\rangle$). Like all TT states it is gapped and thus differs from the gapless bulk state. We will now investigate what happens when the circumference increases from zero and hopping terms start to compete with the electrostatic interaction.

Assume that we are in a regime where the electrostatic repulsion between the particles still plays a major role, such that the low-energy sector consists of states where each pair of sites $(2i, 2i+1)$ contains exactly one particle and one empty site (a copy of this restricted Hilbert space is obtained for the pairs $(2i-1, 2i)$). Every such pair can then be assigned a spin according to

$$n_{2i}, n_{2i+1} = 10 \;\to\; s_i^z = \uparrow, \quad n_{2i}, n_{2i+1} = 01 \;\to\; s_i^z = \downarrow . \tag{2.27}$$

In this way, the many-particle states in this subspace, which we call $\mathcal{H}'_f$, are mapped onto spin-1/2 chains. The mapping is obviously reversible.

The next step is to write down an effective spin hamiltonian that can be analyzed to extract information about the system. Clearly, however, not all hopping terms in Eq. (2.22) preserve $\mathcal{H}'_f$. This means that most hopping operators cannot be expressed in spin notation and in all energy states we will have more or less mixing of states inside and outside the subspace. However, processes involving the shortest-range hopping $\hat{V}_{21}$, which is the dominant hopping term on the thin torus, always preserve the subspace. Because of this and the strong electrostatic repulsion, one may expect that the low-energy states only have negligible contributions from states outside $\mathcal{H}'_f$.

If considering only the electrostatic interaction and hopping processes that preserve the subspace, it is possible to write down a spin hamiltonian

acting within $\mathcal{H}'_f$. One finds

$$\hat{H}'_f = \sum_i \sum_{k=1}^{N_s/4} \Big[\frac{\alpha_k}{2}(s_i^+ s_{i+k}^- + h.c.) + \beta_k s_i^z s_{i+k}^z \Big], \tag{2.28}$$

where $\alpha_k = 2V_{2k,1}$, and $\beta_k = 2V_{2k,0} - (1 - \delta_{k,N_s/4})V_{2k+1,0} - V_{2k-1,0}$. The method for achieving this expression is to consider the terms in (2.22) which preserve $\mathcal{H}'_f$ and figure out how spin operators would act on the corresponding spin states to give the same effect. To get the correct factors in front of the electrostatic terms, it is useful to apply $n_{2i} = \frac{1}{2} + s_i^z$, $n_{2i+1} = \frac{1}{2} - s_i^z$, which follows directly from the mapping rules in (2.27).

Clearly, the spin flips in (2.28) correspond to hopping and the Ising terms correspond to electrostatics. The fact that $V_{2k,1}$ is the only hopping coefficient represented reflects that all hopping operators but $\hat{V}_{2k,1}$ take any spin state out of the subspace—or, is not even defined within the same. $\hat{V}_{2k,1}$, on the other hand, act within the subspace by flipping spins:

$$|...01...10...\rangle \leftrightarrow |...10...01...\rangle \;\Leftrightarrow\; |...\downarrow...\uparrow...\rangle \leftrightarrow |...\uparrow...\downarrow...\rangle. \tag{2.29}$$

Specifically, the shortest hopping equals the nearest-neighbor spin flip,

$$\hat{V}_{21} = V_{21} \sum_i (s_i^+ s_{i+1}^- + h.c.) = \frac{\alpha_1}{2} \sum_i (s_i^+ s_{i+1}^- + h.c.). \tag{2.30}$$

When L_1 is small enough, the hopping amplitudes α_k are essentially zero and Eq. (2.28) tells us that the ground states are the spin-polarized TT states $|\uparrow\uparrow\uparrow\uparrow...\rangle = [10]$ and $|\downarrow\downarrow\downarrow\downarrow...\rangle = [01]$, as long as $\beta_k < 0$, which holds for all convex[6] interactions like Coulomb and screened Coulomb. However, as L_1 grows we shall expect the hopping coefficients α_k to become more dominant and numerical calculations show that between $L_1 \sim 5$ and $L_2 \sim 8$ it is a valid approximation to write

$$\hat{H}'_f \approx \frac{\alpha_1}{2} \sum_i (s_i^+ s_{i+1}^- + h.c.). \tag{2.31}$$

This hamiltonian describes the so-called XY spin chain. It is exactly solvable in terms of free neutral dipoles and the system is as such gapless. The ground state is homogeneous, consisting of the very "hoppable" (with $\hat{V}_{21}$) state $|11001100...\rangle = |\uparrow\downarrow\uparrow\downarrow...\rangle$ and all kinds of spin flips on this. Since

[6] Convex here means that $V''_k \equiv V_{k+1,0} + V_{k-1,0} - 2V_{k,0} > 0 \; \forall k$.

approximations have been made, this will never be the exact ground state of the full hamiltonian, but one may expect that as long as the deviations are sufficiently small, the system remains in a gapless phase.

The above can be illustrated by a simple phase diagram, see Fig. 2.5, with the torus circumference on the x-axis. Exact diagonalization for a limited number of particles shows [22] that for very thin tori, the ground state at $\nu = 1/2$ is the crystal $|1010...\rangle$. At $L_1 \approx 5.3$, however, there is a phase transition to a homogeneous state (the XY phase), with contributions from the hoppable $|1100...\rangle$.

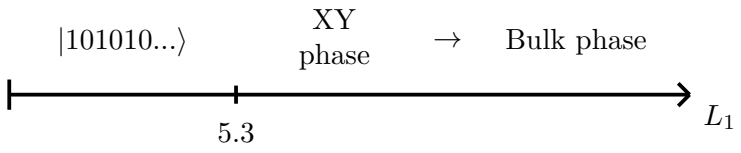

Figure 2.5: *An approximate phase diagram for fermions at $\nu = 1/2$ and Coulomb interaction as a function of L_1. Figure originally by E.J. Bergholtz, borrowed from Paper III.*

As L_1 becomes so large that other hopping terms than $\hat{V}_{21}$ become important, the truncation in Eq. (3.2) and, hence, the exact solution are no longer valid. However, numerics suggests that the XY phase evolves continuously towards the bulk system as $L_1 \to \infty$, indicating that the description to some extent is relevant also for the real experimental system. Even more interesting for our coming purposes, analyses suggest that for gapless and non-abelian QH states in general, the infinitely thin torus and the bulk are separated by exactly one phase transition, whereas for abelian QH states, the ground state of the infinitely thin torus evolves continuously to the bulk state.[7] In both cases the thin torus contains much of the physics of the experimental system. In light of the above, the rest of this thesis will treat various quantum Hall states, as well as other effectively one-dimensional lattice systems from a thin-torus perspective. Our first example is another half-filled system, namely the non-abelian $\nu = 5/2$, and the analysis is to a large extent inspired by and related to the earlier findings on $\nu = 1/2$.

[7]The latter follows from the analytical and numerical studies of the Laughlin wave function for $\nu = 1/3$ on the thin cylinder by Rezayi and Haldane [26], as pointed out in [25]. See also [27].

Chapter 3

Fermions at $\nu = 5/2$

In Section 2.4 we reviewed one of the first applications of the thin-torus view on a concrete physical system, namely the gapless $\nu = 1/2$. There, the low-energy sector was mapped onto spin-1/2 chains through

$$n_{2i}, n_{2i+1} = 10 \;\rightarrow\; s_i^z = \uparrow, \quad n_{2i}, n_{2i+1} = 01 \;\rightarrow\; s_i^z = \downarrow, \tag{3.1}$$

and the resulting spin hamiltonian

$$\hat{H}'_f = \sum_i \sum_{k=1}^{N_s/4} \Big[\frac{\alpha_k}{2} (s_i^+ s_{i+k}^- + h.c.) + \beta_k s_i^z s_{i+k}^z \Big], \tag{3.2}$$

where $\alpha_k = 2V_{2k,1}$, and $\beta_k = 2V_{2k,0} - (1 - \delta_{k,N_s/4})V_{2k+1,0} - V_{2k-1,0}$. The interaction parameters α_k and β_k correspond to hopping and electrostatic interaction, respectively. For very small values of L_1, the electrostatic terms dominate and the ground state is the spin-polarized TT state. For larger values of L_1 this state is replaced by the gapless XY spin chain, which minimizes the nearest-neighbor hopping term with coefficient α_1. In this chapter we will build on this knowledge by investigating a very different system using the same spin mapping. For further reading related to the contents of this chapter, see Papers I and III.

3.1 Half-filling revisited and extended

Experiments show that the quantum Hall system at half-filling in the second Landau level, $\nu = 5/2$, is gapped, unlike half-filling in the lowest Landau level. Furthermore, theoretical studies suggest that it has a sixfold ground

state degeneracy, as opposed to the trivial twofold center-of-mass degeneracy, and that it supports fractional excitations of charge $e^* = \pm e/4$ which obey non-abelian statistics (see Section 1.3.3). We saw earlier that the creation of fractional charges $e^* = \pm e/2$ in the thin limit at half-filling is a simple consequence of the twofold degeneracy of the TT ground state. The appearance of $\pm e/4$ charges at $\nu = 5/2$, on the other hand, is a highly nontrivial phenomenon.

In 1991, Moore and Read [28] wrote down a many-particle wave function that is believed to describe the $\nu = 5/2$ system well. The function, called the Moore-Read (MR), or pfaffian, wave function, is the exact ground state of a repulsive three-body interaction [29,30] that prevents triples of electrons to be close to each other. On the thin torus this is manifested in six degenerate ground states of the types $|1010...\rangle$ and $|1100...\rangle$. (Note that these are the only lattice states with at most two particles on any three consecutive sites.) In the real physical system, of course, the electrons are interacting not via some strange three-body interaction, but via ordinary two-body repulsion, just like at half-filling in the lowest Landau level. The physical differences between the two systems are derivates of the different single-particle wave functions occupied by the electrons. For $\nu = 1/2$ these are ψ_{0k}, while for $\nu = 5/2$ they are ψ_{1k}.

Now, note that both $|1010...\rangle$ and $|1100...\rangle$ are contained in the subspace $\mathcal{H}'_f$, defined in Section 2.4, since their sites can be divided into pairs where each pair contains exactly one particle. It thus seems plausible that the physics of the pfaffian system might as well be captured by the spin mapping introduced for $\nu = 1/2$. Obviously, since $\nu = 5/2$ is gapped, the gapless XY chain is not a valid description—however, other terms in the spin hamiltonian might become dominant as a consequence of the effective interaction in the second Landau level.

Let us do a numerical calculation of the behavior of the interaction parameters α_k and β_k in Eq. (2.28) as the torus circumference L_1 is varied—first for $\nu = 1/2$ and then for $\nu = 5/2$.

In Fig. 3.1 we have plotted the largest coefficients α_k and β_k for $\nu = 1/2$ between $L_1 = 4$ and $L_1 = 8$, for Coulomb as well as for a short-range interaction $\nabla^2\delta$. We see that as L_1 decreases, the hopping terms α_1 and α_2 tend to zero as expected; the hamiltonian is dominated by the electrostatic repulsion. In this thin-limit regime the TT state is the ground state of the lattice system, as concluded earlier. However, going to the right in the diagram we see how the shortest hopping coefficient α_1 grows and around

$L_1 \sim 5$ it is actually the dominant one.[1] This should not surprise us—we have already stated that Eq. (3.2) is a valid approximation in a regime from around $L_1 \sim 5.3$, where the phase transition to the gapless phase occurs.

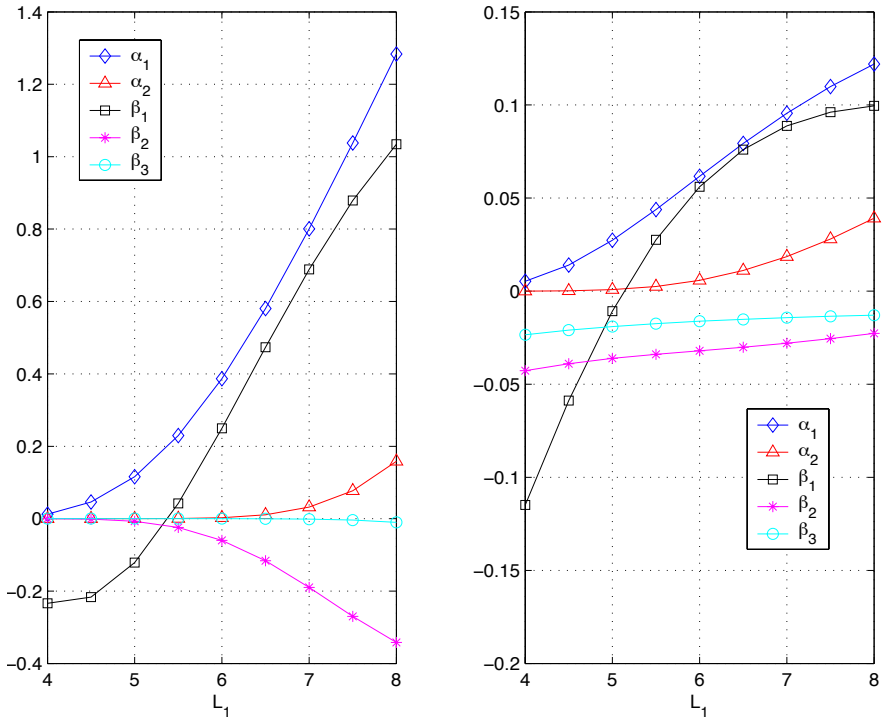

Figure 3.1: *Plots showing the largest coefficients in the spin chain hamiltonian for half-filling in the lowest Landau level, short-range interaction, $V(\mathbf{r}) = \nabla^2\delta(\mathbf{r})$ (left), and Coulomb interaction (right), respectively. This specific plot is constructed for $N_s = 16$ but varying the system size does not change the appearance significantly. Figure by E.W., borrowed from Paper III.*

Let us compare these results with the corresponding ones for $\nu = 5/2$ by reconstructing the plot in Fig. 3.1 for Coulomb in the *second* Landau level, being displayed in Fig. 3.2. We see that as L_1 goes to zero, the system behaves in the same way as $\nu = 1/2$; all hopping terms vanish and we expect the ground state $|1010...\rangle$. However, the graphs differ as we approach the thickness where the nearest-neighbor Ising term is small compared to

[1]For Coulomb interaction (right panel), this is not obvious from the graph but, as mentioned in Section 2.4, numerics strongly suggests that this is the case.

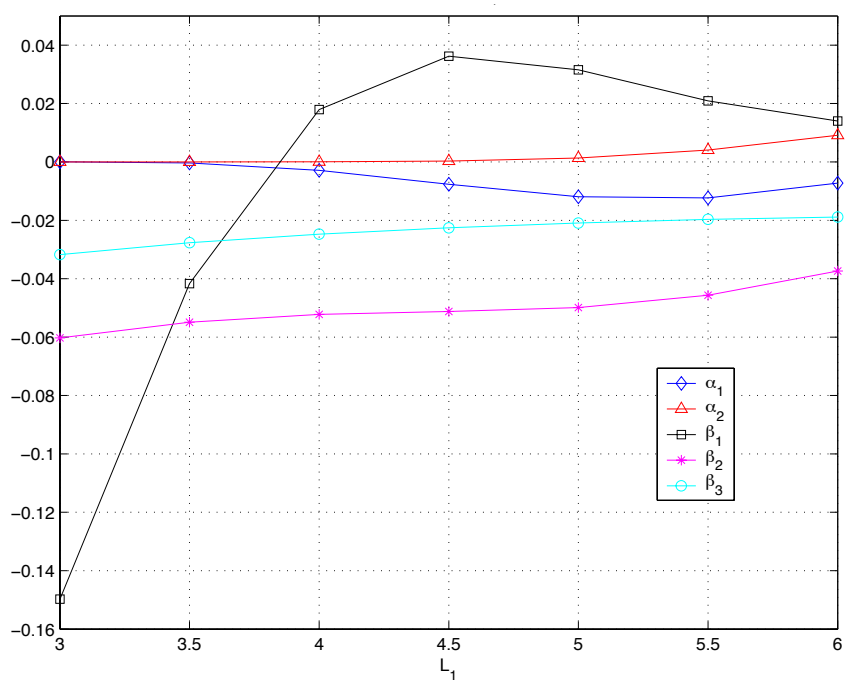

Figure 3.2: *Plot showing the largest coefficients in the spin chain hamiltonian for half-filling in the second Landau level, Coulomb interaction. These specific plots are constructed for $N_s = 16$ but varying the system size does not change the appearances significantly. Figure by E.W., borrowed from Paper III.*

the shortest hopping. Here, when $\beta_1 \approx 0$, the electrostatic coefficient β_2 remains quite large compared to α_1. It is interesting to reflect on what the consequences of truncating the hamiltonian to

$$\hat{H}'_f \approx \beta_2 \sum_i s_i^z s_{i+2}^z, \tag{3.3}$$

$\beta_2 < 0$, would be. Obviously, the energy is in this case minimized by all spin states where all pairs of next-nearest neighbors have the same spin, i.e., we get the six exactly degenerate ground states $|\,1\,\rangle = |\uparrow\uparrow\uparrow\uparrow ...\rangle$, $|\,\tilde{1}\,\rangle = |\downarrow\downarrow\downarrow\downarrow ...\rangle$, $|\,2\,\rangle = |\downarrow\uparrow\downarrow\uparrow ...\rangle$ and $|\,\tilde{2}\,\rangle = |\uparrow\downarrow\uparrow\downarrow ...\rangle$, which exactly correspond to the pfaffian states when translated to number representation.[2]

[2]The states $|\,2\,\rangle$ and $|\,\tilde{2}\,\rangle$ have inequivalent copies in the other choice of subspace, while the states $|\,1\,\rangle$ and $|\,\tilde{1}\,\rangle$ have only equivalent copies. Hence, there are six states in total.

While the hamiltonian in (3.3) is minimized by the states where all pairs of next-nearest-neighbors have the same spin, a minimal excitation is created by letting two pairs of next-nearest neighbors have opposite spins[3], which in turn is accomplished by constructing domain walls between the various ground states. Furthermore, these excitations increase the energy of the state by $-\beta_2$, i.e., there is a gap.[4] Examples of states with minimal excitations are given here:

$$|\uparrow\uparrow\uparrow\uparrow\uparrow\uparrow\uparrow\uparrow\uparrow\uparrow\downarrow\uparrow\uparrow\uparrow\uparrow\uparrow\uparrow\uparrow\uparrow\uparrow\uparrow\rangle,$$
$$|\uparrow\uparrow\uparrow\uparrow\uparrow\uparrow\uparrow\uparrow\uparrow\downarrow\uparrow\downarrow\uparrow\downarrow\uparrow\uparrow\uparrow\uparrow\uparrow\uparrow\uparrow\uparrow\rangle,$$
$$|\uparrow\uparrow\uparrow\uparrow\uparrow\uparrow\uparrow\downarrow\uparrow\downarrow\uparrow\downarrow\uparrow\downarrow\uparrow\downarrow\uparrow\uparrow\uparrow\uparrow\uparrow\uparrow\uparrow\rangle.$$

When the domain wall excitations are translated into number representation, it becomes clear that the quasiholes/-particles carry fractional charge $e^* = \pm\frac{e}{4}$. As an example, consider the state

$$|\uparrow\uparrow\underline{\uparrow}\uparrow\underline{\downarrow}\uparrow\downarrow\uparrow\underline{\downarrow}\uparrow\underline{\uparrow}\uparrow\uparrow\uparrow\rangle = |10101\underline{0100}1100110\underline{1101}0101010\rangle.$$

Here, the blue-colored and underlined pair of opposite spins translates into the blue-colored string of four consecutive sites containing only one particle instead of two. This is a $-e/4$ charge. The red-colored and underlined sequence is, analogously, an $e/4$ charge.

Summarizing the findings presented in this section, one may conclude that the difference in size of the β_2-term between $\nu = 1/2$ and $\nu = 5/2$ has part in why the latter realizes the pfaffian (and not a gapless) phase on the thin torus.

3.2 A phase diagram for half-filling

The difference in behavior between $\nu = 1/2$ and $\nu = 5/2$ is due to the fact that the interaction parameters V_{km} depend on the single-particle wave functions ψ_{nk}; the same potential $V(\mathbf{r})$ produces different effects together with ψ_{0k}, and ψ_{1k}, respectively, see Eq. (2.20) and Figs. 3.1, and 3.2. Of

[3]Note that this holds when periodic boundary conditions are assumed. Otherwise a single pair of opposite spin would be possible and, hence, that would be the minimal excitation.

[4]In the ground state, all pairs have energy $\beta_2/4$. In an excited state, two pairs have opposite spin, each with energy $-\beta_2/4$. Hence the difference in energy compared to the ground state is $-\beta_2$.

course, different kinds of phases can alternatively be produced by changing the inter-particle potential while keeping the single-particle functions invariant. In fact, through the use of a so-called pseudopotential expansion, the physics of the second Landau level can be mimicked using the lowest-Landau-level wave functions. This also allows for an investigation of the stabilities of $\nu = 1/2$ and $\nu = 5/2$, since the potential can be varied continuously.

The pseudopotential method

The method of studying the quantum Hall system using pseudopotentials was invented by Haldane in the 1980's [31]. The idea is to make a kind of Taylor expansion of the potential and vary the expansion parameters. The hamiltonian of any two-body interaction can be written as

$$\hat{H} = \sum_{i<j} \sum_{m=0}^{\infty} V_m \hat{P}_m(M_{ij}), \tag{3.4}$$

where $\hat{P}_m(M_{ij})$ projects onto a state where particles i and j have relative angular momentum m. V_m are the pseudopotential parameters, which are real numbers determined by the specific interaction:

$$V_m = \int_0^{\infty} q\tilde{V}(q) L_m(q^2) e^{-q^2} dq, \tag{3.5}$$

where $\tilde{V}(q)$ is the Fourier transform of the potential and L_m are the Laguerre polynomials $L_0(q^2) = 1$, $L_1(q^2) = 1-q^2$,... For Coulomb interaction, $\tilde{V}(q) = \frac{1}{q}$.

By varying one or several pseudopotential parameters, i.e., letting $V_m \to V_m + \delta V_m$, one can simulate new kinds of interactions. Here, we will start from V_{km} as given by Coulomb interaction and the single-particle wave functions of the lowest Landau level ($\nu = 1/2$), and vary them to yield new states, corresponding to Coulomb interaction in the second Landau level ($\nu = 5/2$).

Recall from Eq. (2.23) that V_{km} is determined by $V_{k_1 k_2 k_3 k_4}$, which in turn is determined by $\tilde{V}(\mathbf{q})$ through Eq. (2.21). We will vary V_{km} by adding a small term δV_1 to the first pseudoparameter: $V_1 \to V_1 + \delta V_1$, which is equivalent to

$$\tilde{V}(\mathbf{q}) = \frac{1}{q} \;\to\; \frac{1}{q} + 2\delta V_1(1 - q^2). \tag{3.6}$$

The Fourier-space potential $\delta\tilde{V}(\mathbf{q}) = 2\delta V_1(1-q^2)$ corresponds to a real-space interaction on the form

$$\delta V(\mathbf{r}) = 2\delta V_1(1 + \nabla^2)\delta(\mathbf{r}). \tag{3.7}$$

The choice to add this short-range interaction term to the hamiltonian is motivated by the fact that short-range interactions are known to play a crucial role in quantum Hall systems.[5] Since we are dealing with fermions, the delta function $\delta(\mathbf{r})$ will have no effect on the matrix elements. However, $\nabla^2\delta(\mathbf{r})$ gives rise to a positive potential energy for a pair of particles very close to each other[6], so adding this term to the hamiltonian will favor states where the probability for electrons to come close is small. In contrast, a negative sign in front of $\nabla^2\delta(\mathbf{r})$ will lower the energy of pairs of closely lying electrons relative to the Coulomb case.

We are searching for the pfaffian ground states, which we know are exact ground states of a repulsive three-body interaction that separates all triples of particles. On the thin torus they are the crystalline states $[10] = |1010...\rangle$ and $[1100] = |11001100...\rangle$, and their translations. We know that [10] is the ground state for Coulomb interaction at half-filling in the thin limit, whereas [1100] is a state that obviously is favored by a potential that allows for pairs of electrons to be close to each other. A guess is therefore that one should choose negative values of δV_1 and thus add a negative $\nabla^2\delta(\mathbf{r})$ to the potential to find the $\nu = 5/2$ phase. Note that small values of δV_1 will let the repulsive Coulomb term remain important.

A phase diagram for half-filling

Fig. 3.3 shows a phase diagram[7] for half-filling, with the pseudopotential parameter δV_1 on the y-axis and the torus circumference L_1 on the x-axis. A computer program for exact diagonalization of small systems (here, eight particles) has been used to find the ground states at various points in the diagram.

For ordinary Coulomb interaction in the lowest Landau level, i.e., for $\delta V_1 = 0$, we find the phases of $\nu = 1/2$. Up to $L_1 \sim 5.3$, the ground state is the state evolving from the crystalline state $|1010101010101010\rangle$[8]. At

[5] For example, the Laughlin wave functions are exact ground states when only the first expansion terms in (3.4) are non-vanishing.

[6] One can show by partial integration that the expectation value of $\nabla^2\delta(\mathbf{r})$ is nonzero. Although the wave function Ψ must go to zero for $\mathbf{r}_i = \mathbf{r}_j$, there is no such constraint on $\nabla\Psi$.

[7] Phase diagrams are usually studied in thermodynamics and require, strictly speaking, the number of particles to be infinite. However, previous experience of analyzing quantum Hall systems has shown that even systems of very few particles provide a fairly accurate picture of the system in the thermodynamic limit.

[8] Again, we disregard half of the states and just remember that there is a trivial twofold translational degeneracy of every state.

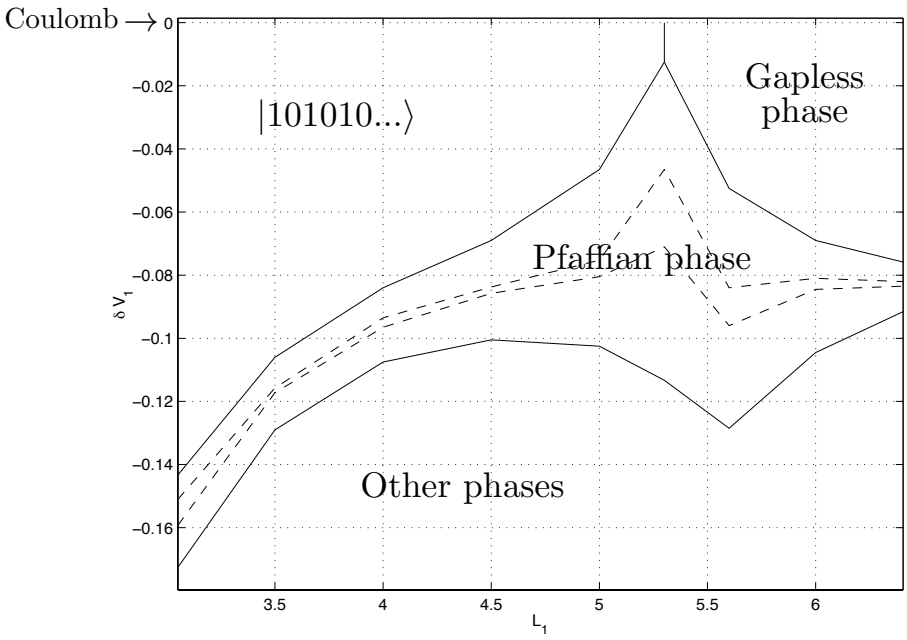

Figure 3.3: *Phase diagram for half-filling as a function of L_1 and δV_1. At $\delta V_1 = 0$ (Coulomb interaction in the lowest Landau level), the crystalline state $|1010...\rangle$ is separated from the gapless phase at $L_1 \sim 5.3$. Within the solid lines in the middle, the pfaffian states are lowest in energy, and within the dashed lines their mutual energy difference is less than 10% of the gap to the next excited state, meaning that they are close to degenerate. Figure by E.W., borrowed from Paper I.*

$L_1 \sim 5.3$ there is a phase transition to the state described by the gapless phase of neutral dipoles, as discussed in Section 2.4. Note from the phase diagram that the ground states at $\nu = 1/2$ are quite robust against changes in the interaction.

As the pseudopotential parameter is decreased from zero, we eventually get to a regime where the pfaffian states are lowest in energy. This area is labeled 'Pfaffian phase' in Fig. 3.3. The phase is identified by following the lattice states $|1010...\rangle$ and $|1100...\rangle$ from the very thin torus towards larger L_1, where they lose their simple crystalline nature but keep their quantum numbers. The thin-torus states can be thought of as "parents" of the corresponding pfaffian bulk states.

Note that the pfaffian phase is reached much earlier around the $\nu = 1/2$

phase transition than on the very thin torus in the leftmost part of the diagram. This is explained by the fact that, at the phase transition, both the TT state $|1010...\rangle$ and the XY phase (the latter related to the pfaffian state $|1100...\rangle$), have low energy. Hence, the potential does not need to change very much until the regime where these states are degenerate is reached. On the other hand, on the very thin torus the TT state $|1010...\rangle$ is the unique ground state even in the second Landau level. Thus, as the torus becomes thinner, one has to change the interaction more to find the pfaffian phase. As L_1 increases, the pfaffian phase can be followed as it evolves towards the larger system.

Fractional charges

Choosing a point in the phase diagram where the pfaffian phase is dominant, one can study the emergence and evolution of fractional charges in the $\nu = 5/2$ system. Plotting the average particle density at different sites gives a clear picture of the fractional charges, especially on the thin torus. In Fig. 3.4, the ground state at slightly below half-filling is studied for a small number of particles. There, fractional charges should appear in the ground state configuration, not only as excitations.

From the density profile in the figure, one can see that in the thin limit this particular state has the crystalline form $|\underline{0}1100\underline{11}\underline{0010}101\underline{010}\rangle$. Clearly, this ground state consists of alternating domains of the lattice configurations [01] and [0110]. This mixing is possible thanks to the degeneracy of these states in the pfaffian regime. At the interfaces, there are accumulations of positive charge (blue color and underlined in the sequence). The charge of these domain walls can be calculated as follows. In every string of four consecutive sites in the background ground states, there are exactly two particles. At the domain walls, however, one single string of four sites instead contains *one* particle. The change in charge concentration in this deviating string corresponds to an $-e/4$ charge. Note from the density plot that this picture of the origin of the fractional charges seems to hold also for the thicker torus. Indeed, the change in the particle density as L_1 increases indicates that it evolves continuously towards the larger system.

Considering the low-energy spectrum at $N_e = 8$, $N_s = 16$, i.e., exactly at half-filling, in the pfaffian regime, one can also search for fractional charges in excited states. One expects, since the positively and negatively charged quasiparticles attract each other, that the lowest states will keep these charges close together, while they will become more separate in higher excitations. Computer simulations give that the first excited state is of the

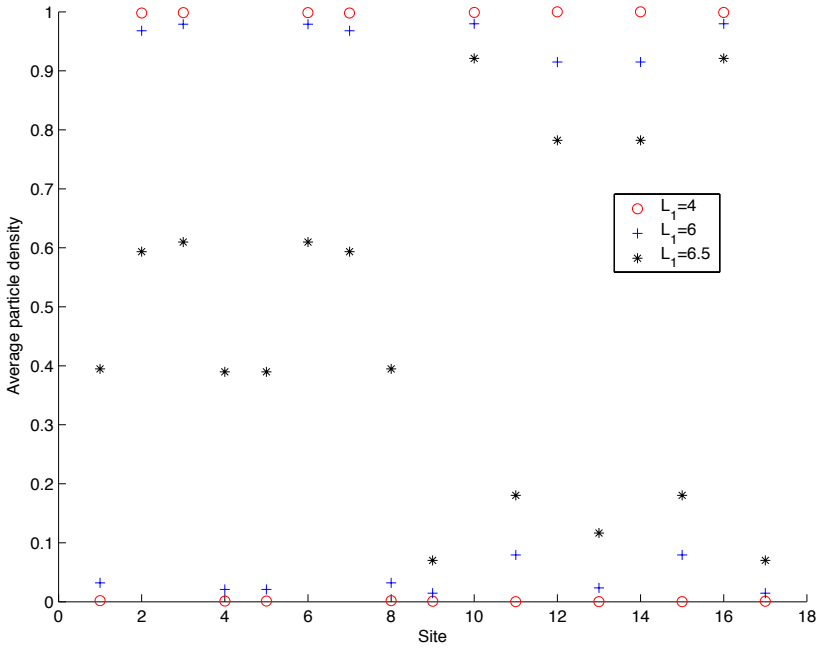

Figure 3.4: *Plot of the particle density at filling fraction* $8/17$ *in the pfaffian regime, site number on the* x*-axis. Here, two fractional charges are formed as domain walls between the crystalline states* $|0110...\rangle$*, and* $|0101...\rangle$*. As* L_1 *grows, the density profile evolves seemingly continuously.*

kind $|1010\underline{1011}\underline{00101}010\rangle$.[9] This state allows for two different interpretations. Either it is seen as the state $[10] = |1010...\rangle$ but with one electron moved one step in the lattice (fractional charges $+e/2$ and $-e/2$ beside each other). Or, one can see it as a string of $[10]$ connected to a short sequence of $[0011] = |0011...\rangle$ and two quarter charges very close to each other at the domain walls (red and blue underlined). A similar situation holds for the second excited state, which looks like $|0110011\underline{00101}\underline{0110}\rangle$. Here, the background state is $[0110]$. In the third excited state, however, the quarter-charged quasiparticles are more evident. This state, $|\underline{1011}00\underline{11}\underline{00101}010\rangle$ clearly consists of alternating strings of $[10]$ and $[0011]$.

[9] The state has a 32-fold degeneracy (16 translations, and mirrored states).

Chapter 4

Bosons at $\nu = 1$

The systems treated so far in this thesis have been fermionic. The wave functions have been antisymmetric and we have only allowed for one particle on each lattice site. However, a somewhat unexpected mathematical connection will now take us from the two-dimensional electron gas to rotating Bose-Einstein condensates (BEC's), more specifically to bosons at filling fraction $\nu = 1$. The contents of the chapter are based on Paper III.

4.1 Rotating BEC's and the quantum Hall effect

A little over a decade ago it was realized that there is an intimate connection between fermions in the quantum Hall system and neutral bosons in rapidly rotating Bose-Einstein condensates [32, 33].[1] It turns out that the hamiltonians for the two cases are mathematically equivalent and so the analysis of the two seemingly very different systems can be unified. Strong magnetic field for fermions here corresponds to high rotational frequency of the BEC.

Experimentally, much progress has been made within the area of Bose-Einstein condensates during the last decade. Very fast rotation speeds have revealed fascinating properties of the rotating condensates, the most striking being regular vortex lattices piercing the samples. However, to get into the quantum Hall regime, even higher frequencies are required—so high that the condensate clouds easily escape the confining potential and fly apart. To this day this problem is not solved, although the experiments are advancing. This does, however, not prevent further theoretical investigations; let us see how this system can be treated in the thin-torus lattice model.

[1] For a nice review of the subject, see [34].

4.1.1 Boson filling fractions and lattice hamiltonians

On the plane, the Laughlin wave function [8] reads

$$\Psi_{\frac{1}{2m+1}}(z_1, z_2, \ldots, z_{N_e}) = \prod_{i<j}(z_i - z_j)^{2m+1} e^{-\frac{1}{4}\sum_i |z_i|^2}. \tag{4.1}$$

Here, $z = x + iy$ and (x, y) are the particle coordinates in the plane. The numbers 1 to N_e label the electrons and $J = \prod_{i<j}(z_i - z_j)$ is called the *Jastrow factor*. Note that the polynomial factor J^{2m+1} makes this an anti-symmetric, fermionic wave function. This trial wave function is an extremely good approximation to the quantum Hall ground state at $\nu = \frac{1}{2m+1}$, and it predicts both the expected gap and excitations with fractional charge $e^* = \pm\frac{e}{2m+1}$.

There is a bosonic counterpart of the Laughlin wave function, namely $\Psi_{\frac{1}{2m}} \sim J^{2m}$, which is symmetric in the particle coordinates. If this symmetric wave function is multiplied by another Jastrow factor, the filling changes: $\nu = \frac{1}{2m} \to \frac{1}{2m+1}$, and the fermionic Laughlin function is restored; we have gone from bosons at filling $\nu = \frac{1}{2m}$ to fermions at filling $\nu = \frac{1}{2m+1}$. Considering this connection one finds it probable to find similarities between fermions at filling $\nu = 1/2$ and bosons at filling $\nu = 1$. However, whereas the fermionic system as we know realizes a gapless metallic state, the bosonic counterpart rather seems to be described by a threefold degenerate pfaffian Moore-Read wave function [28], making it more similar to fermions at $\nu = 5/2$. This has been indicated by numerical studies [35–37].

When considering the one-dimensional lattice picture of the bosonic system, we must remember that interchanging two particles gives a plus sign, and allow for the possibility for two particles to hop to or from the same site. Equation (2.22) and (2.23) shifts into

$$\hat{H} = \sum_i \sum_{|m|\le k\le N_s/2} V_{km} b^\dagger_{i-k} b^\dagger_{i+m} b_{i-k+m} b_i =$$

$$= \sum_i \sum_{0\le m\le k\le N_s/2} V_{km} b^\dagger_{i-k} b^\dagger_{i+m} b_{i-k+m} b_i + h.c. \equiv \sum_{0\le m\le k\le N_s/2} \hat{V}_{km} \tag{4.2}$$

and

$$V_{km} = \frac{1}{2^{\delta_{k,m}(1+\delta_{k,0})} 2^{\delta_{k,N_s/2}}} (V_{i+m,i+k,i+m+k,i} + V_{i+m,i+k,i,i+m+k} + V_{i+k,i+m,i,i+m+k} + V_{i+k,i+m,i+m+k,i}). \tag{4.3}$$

Also note that for bosons, no Landau level is ever filled or inert because many bosons may occupy the same single-particle state. For the same reason,

provided that the rotational frequency of the sample is high enough, only the lowest Landau level will be occupied, even for $\nu > 1$. Considering these facts we may now seek a thin-torus description of the rotating bosons.

4.2 Mapping of $\nu = 1$ onto spin-$1/2$ chains

In the previous chapter we mapped a half-filled Landau level onto spin-1/2 chains, an approach which assisted with a simplified view of $\nu = 1/2$ and $\nu = 5/2$. Here, we will apply the same mapping (although in a bit more complicated manner) to bosons at filling $\nu = 1$.

4.2.1 Low-energy subspace and mapping rules

Consider only states where every n consecutive sites contain from $n-1$ to $n+1$ particles. In other words, disallow states where a single site hosts more than two particles, as well as states which contain strings of the kind 011...110, and 211...112. This restriction is favorable from an electrostatic point of view; the subspace $\mathcal{H}_b'$ consisting of the allowed states should make a good definition of a low-energy sector on the thin torus.[2] Now, let every site in the original boson state split into two new sites, $(2i-1, 2i)$, on which the number of particles divide:

$$\begin{cases} n_i = 2 & \rightarrow & n'_{2i-1}, n'_{2i} = 11 \\ n_i = 0 & \rightarrow & n'_{2i-1}, n'_{2i} = 00 \\ n_i = 1 & \rightarrow & n'_{2i-1}, n'_{2i} = 10 \text{ or } 01. \end{cases} \tag{4.4}$$

The mapping of $n_i = 1$ is determined by the occupation number on neighboring sites. If $n_{i-1} = 2$, then $n_i = 1 \rightarrow n'_{2i-1}, n'_{2i-1} = 01$, whereas if $n_{i-1} = 0$, then $n_i = 1 \rightarrow n'_{2i-1}, n'_{2i-1} = 10$. If $n_{i-1} = 1$, then n_i is mapped in the same way as n_{i-1}, so that the mapping of entire strings ...11111... depends on whether there is a 0 or a 2 at the left end of the string. Finally, let the state $|1111...\rangle \rightarrow |01010101...\rangle \equiv |10101010...\rangle$ for completeness. As an example,

$$|112111011\rangle \rightarrow |101011010101001010\rangle.$$

Note that the lattice states one gets after the splitting of each site obviously have filling fraction $\nu = 1/2$. Moreover, they fulfill the restriction

[2] On the thick torus, hopping will make contributions from states outside of $\mathcal{H}_b'$ too large for this subspace to cover the low-energy sector. Numerics indicate that it is a good choice of subspace up to $L_1 \sim 6$.

that every pair of sites $(2i, 2i+1)$, $i = 1, 2, ...$, contains exactly one particle. The only difference between this and the fermionic subspace $\mathcal{H}'_f$ is that the alternative pairing of sites, $(2i-1, 2i)$, is not allowed here because $n'_{2i-1}, n'_{2i} = 11$ for $n_i = 2$, and $n'_{2i-1}, n'_{2i} = 00$ for $n_i = 0$. Let us make the mapping complete by imposing

$$n'_{2i}, n'_{2i+1} = 10 \ \rightarrow \ s_i^z = \uparrow, \quad n'_{2i}, n'_{2i+1} = 01 \ \rightarrow \ s_i^z = \downarrow, \tag{4.5}$$

as before. In other words, $s_i^z = \frac{1}{2}(n'_{2i} - n'_{2i+1})$. Note that domain walls between spin-polarized sections are found wherever there were 0's and 2's in the original boson state. Returning to the example above, we have

$$|112111011\rangle \ \rightarrow \ |101011010101001010\rangle \ \rightarrow \ |\downarrow\downarrow\uparrow\uparrow\uparrow\uparrow\downarrow\downarrow\downarrow\rangle.$$

By reversing the mapping, every given spin chain is uniquely mapped onto a boson state:

$$s_i^z = \uparrow \ \rightarrow \ n'_{2i}, n'_{2i+1} = 10, \quad s_i^z = \downarrow \ \rightarrow \ n'_{2i}, n'_{2i+1} = 01, \tag{4.6}$$

or, equivalently, $n'_{2i} = \frac{1}{2} + s_i^z$, $n'_{2i+1} = \frac{1}{2} - s_i^z$. Then,

$$\begin{cases} n'_{2i-1}, n'_{2i} = 11 & \rightarrow \quad n_i = 2 \\ n'_{2i-1}, n'_{2i} = 00 & \rightarrow \quad n_i = 0 \\ n'_{2i-1}, n'_{2i} = 10 \text{ or } 01 & \rightarrow \quad n_i = 1. \end{cases} \tag{4.7}$$

These equations are summarized by

$$n_i = n'_{2i-1} + n'_{2i} = 1 + s_i^z - s_{i-1}^z. \tag{4.8}$$

4.2.2 Spin-operator hamiltonian

After having mapped the boson states onto spin states, we need to do the same thing with the hamiltonian by expressing at least the most important terms in (4.2) in terms of spin operators. Keeping the electrostatic interaction and only those hopping terms that preserve $\mathcal{H}'_b$, we find [38] that

$$\hat{V}_{km} = 2^{-\delta_{km}(1-\delta_{m,N_s/2})/2} V_{km} \sum_i s_{i-k}^+ \dots s_{i-k+m-1}^+ s_i^- \dots s_{i+m-1}^-$$
$$\times \sqrt{\frac{3}{2} - s_{i-k-1}^z} \sqrt{\frac{3}{2} + s_{i-k+m}^z} \sqrt{\frac{3}{2} - s_{i-1}^z} \sqrt{\frac{3}{2} + s_{i+m}^z} + h.c., \ m > 0, \tag{4.9}$$

and

$$\hat{V}_{k0} = V_{k0} \sum_i \Big(2 s_i^z s_{i+k}^z - s_i^z s_{i+k-1}^z - s_i^z s_{i+k+1}^z \Big). \tag{4.10}$$

The mapping of the boson states is non-local in the sense that the spin corresponding to $n_i = 1$ can depend on the particle number many sites away. This is why entire domains of spins are flipped in Eq. (4.9).[3]

Note that, just like for fermions, the shortest hopping—$\hat{V}_{11}$ for bosons—corresponds to a nearest-neighbor spin flip:

$$\hat{V}_{11} = \sqrt{2}V_{11}\sum_i \sqrt{\frac{3}{2} - s^z_{i-2}}\sqrt{\frac{3}{2} + s^z_{i+1}}(s^+_i s^-_{i+1} + h.c.) =$$
$$= V_{11}\sum_i \left(\frac{4+3\sqrt{2}}{4} + \frac{1}{\sqrt{2}}(s^z_{i+1} - s^z_{i-2}) + (4-3\sqrt{2})s^z_{i-2}s^z_{i+1}\right)$$
$$\times(s^+_{i-1}s^-_i + h.c.), \quad (4.11)$$

where we have used $s^z_{i-1} = -1/2$ and $s^z_i = 1/2$ for $k = m$, and $(s^z_i)^2 = 1/4$. In contrast to the fermionic case, the shortest hopping here does not in general preserve $\mathcal{H}'_b$. For example, acting with $\hat{V}_{11}$ on any pair of particles in $|1111...\rangle$ creates a site containing three particles, which is not allowed.[4] This *could* imply that $\mathcal{H}'_b$ is not a valid low-energy subspace, even on the thin torus. However, numerics indicate that it is valid after all; there are large overlaps between the ground state of the full hamiltonian and the one restricted to $\mathcal{H}'_b$ in the regime we will be interested in.

At this point it does not seem that we have simplified the problem much. Luckily, however, it turns out that many of the terms in (4.9) and (4.10) may be neglected and it is possible to write the bosonic spin hamiltonian on a form very similar to Eq. (2.28). One finds [38]

$$\hat{H}'_b = \sum_i \sum_{k=1}^{N_s/2} \left[\frac{\alpha_k}{2}(s^+_i s^-_{i+k} + h.c.) + \beta_k s^z_i s^z_{i+k}\right] + \mathcal{O}(s^3), \quad (4.12)$$

where

$$\beta_k = 2V_{k0} - (1 - \delta_{k,N_s/2} + \delta_{k+1,N_s/2})V_{k+1,0} - (1+\delta_{k,1})V_{k-1,0}, \quad (4.13)$$

$$\alpha_1 = \frac{1}{2}\Big(4 + 3\sqrt{2}\Big)V_{11}, \quad (4.14)$$

and

$$\alpha_k = \frac{1}{8}\Big(17 + 12\sqrt{2}\Big)V_{k1}, \ k = 2, 3, \ldots. \quad (4.15)$$

[3] The factors and terms containing s^z_i originate from the factors appearing when the boson operators $b^\dagger$ and b act on states in $\mathcal{H}'_b$, see Eq. (4.2).

[4] Actually, the TT state is special in the sense that *any hopping at all* takes it out of $\mathcal{H}'_b$.

4.3 Ground states and minimal excitations on the thin torus

Considering Eq. (4.12), a natural step is to investigate the relative sizes of the coefficients in the hamiltonian to see if further truncation is possible. Repeating the procedure from Section 3.1, we plot the leading coefficients as functions of L_1 in Fig. 4.1. Like they should, the hopping terms α_k vanish

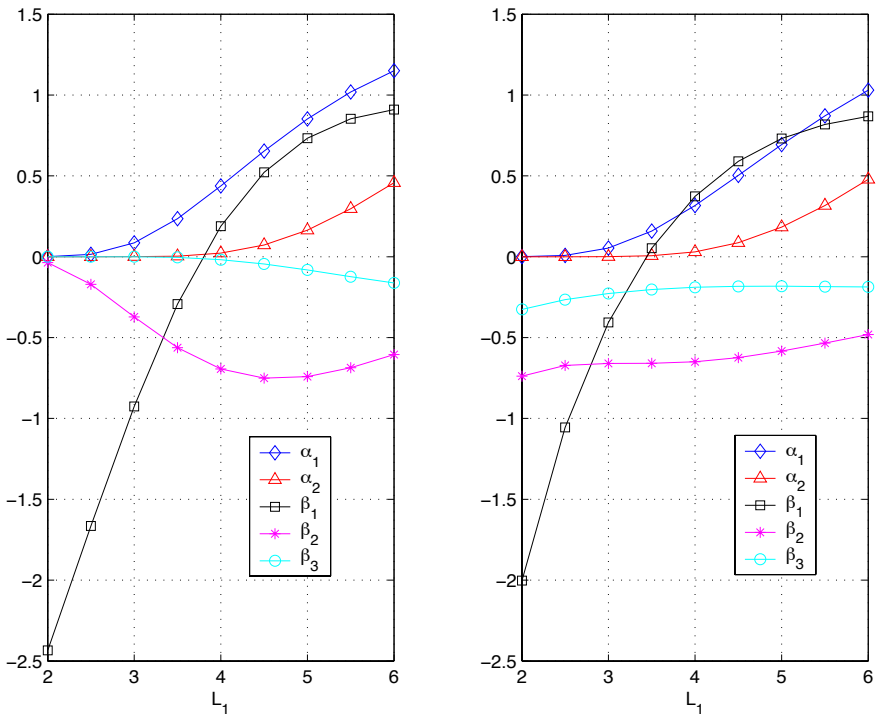

Figure 4.1: *The values of the leading coefficients in the spin chain hamiltonian for bosons at $\nu = 1$ with delta and Coulomb interaction respectively. The plot is constructed for $N_s = 10$, but changing the system size does not change the curves significantly. Figure by E.W., borrowed from Paper III.*

as $L_1 \to 0$. As the circumference increases a bit from zero, the behavior shows in comparison more resemblance to the quantum Hall system $\nu = 5/2$ than to $\nu = 1/2$ (c.f. Figs. 3.1 and 3.2); the hopping coefficient α_1 is

not obviously dominating[5]. Rather, the next-nearest neighbor Ising term β_2 grows large. Let us try a bold approximation and keep only the term $\beta_2 < 0$:

$$\hat{H}_b' \approx \beta_2 \sum_i s_i^z s_{i+2}^z. \tag{4.16}$$

This hamiltonian is minimized by the spin states where every pair of next-nearest neighbors have their spins pointing in the same direction—there are three degenerate ground states: $|\,1\,\rangle = |\uparrow\uparrow\uparrow\uparrow ...\rangle \equiv |\downarrow\downarrow\downarrow\downarrow ...\rangle$, $|\,2\,\rangle = |\downarrow\uparrow\downarrow\uparrow ...\rangle$, and $|\,\tilde{2}\,\rangle = |\uparrow\downarrow\uparrow\downarrow ...\rangle$. Note that the two spin-polarized states are mapped onto the same bosonic state and are thus equivalent by definition. Also, remember that, as opposed to $\nu = 5/2$, there is no second copy of the spin subspace here, so only one version each of $|\downarrow\uparrow\downarrow\uparrow ...\rangle$ and $|\uparrow\downarrow\uparrow\downarrow ...\rangle$ exist.

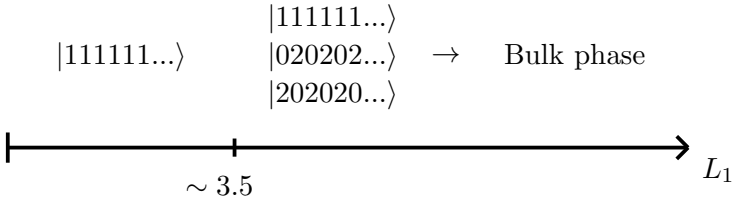

Figure 4.2: *Phase diagram for bosons at $\nu = 1$ and Coulomb interaction as a function of L_1. Figure by E.J. Bergholtz, borrowed from Paper III.*

Interesting things appear when these states are written in number representation. One finds that $|\,1\,\rangle = |1111...\rangle$, $|\,2\,\rangle = |0202...\rangle$ and $|\,\tilde{2}\,\rangle = |2020...\rangle$, which shows agreement with previous knowledge about bosons at $\nu = 1$. These states are, namely, the thin-torus limits of the pfaffian Moore-Read wave function that is believed to describe $\nu = 1$ in the bulk. Furthermore, exact-diagonalization studies on small systems suggest that the truncation we made to arrive at these states is actually rather good within a range on the thin torus above $L_1 \sim 3.5$, see Fig. 4.2. For very small L_1, the TT state $|1111...\rangle$ is the unique ground state. As the torus thickness increases from zero, the states $|2\rangle$ and $|\tilde{2}\rangle$ come closer in energy to the TT state and the three of them are the lowest energy states from around $L_1 \sim 3.5$. At $L_1 \sim 3.8$, $|2\rangle$ and $|\tilde{2}\rangle$ pass the state $|1\rangle$ so that the three are approximately degenerate. They seemingly then evolve continuously towards the

[5]This is, by the way, a reason why the subspace is a good approximation on the thin torus.

thick torus as hopping terms start to influence.[6] To conclude, the very bold truncation in Eq. (4.16) is in good agreement with both the exact diagonalization and the expected Moore-Read ground states within a range of L_1 on the thin torus.

Within this range on the torus, a clear and simple picture of the minimal excitations of the bosonic system at $\nu = 1$ emerges. As we know, the hamiltonian in (4.16) is minimized by states where all pairs of next-nearest neighbors have the same spin. A minimal excitation is created by letting two pairs have opposite spins, which in turn is accomplished by constructing domain walls between different ground states. For example, all states below have the same excitation energy $-\beta_2$:[7]

$$|\uparrow\uparrow\uparrow\uparrow\uparrow\uparrow\uparrow\uparrow\uparrow\uparrow\uparrow\downarrow\uparrow\uparrow\uparrow\uparrow\uparrow\uparrow\uparrow\uparrow\uparrow\uparrow\uparrow\rangle,$$
$$|\uparrow\uparrow\uparrow\uparrow\uparrow\uparrow\uparrow\uparrow\uparrow\uparrow\downarrow\uparrow\downarrow\uparrow\downarrow\uparrow\uparrow\uparrow\uparrow\uparrow\uparrow\uparrow\uparrow\uparrow\rangle,$$
$$|\uparrow\uparrow\uparrow\uparrow\uparrow\uparrow\uparrow\downarrow\uparrow\downarrow\uparrow\downarrow\uparrow\downarrow\uparrow\downarrow\uparrow\uparrow\uparrow\uparrow\uparrow\uparrow\uparrow\uparrow\rangle.$$

When translating these into number representation, one finds that the excitations carry fractional charge $e^* = \pm\frac{e}{2}$.[8] As an example,

$$|\uparrow\uparrow\underline{\uparrow}\uparrow\underline{\downarrow}\uparrow\downarrow\uparrow\underline{\downarrow}\uparrow\underline{\uparrow}\uparrow\uparrow\uparrow\rangle = |111\underline{10}2020\underline{21}111\rangle,$$

where the blue (red) and underlined string is a quasihole (quasiparticle). These fractional excitations are in agreement with the thin-torus limits of the excitations of the bosonic pfaffian wave function [28]. In this picture, they emerge as a consequence of the dominance of the next-nearest neighbor Ising term on the thin torus, acting within the subspace $\mathcal{H}_b'$.

[6] Note that the hopping terms for large L_1 are so dominant that the subspace $\mathcal{H}_b'$ no longer is a valid description of the low-energy sector.

[7] In the ground state, all pairs have energy $\beta_2/4$. Here, we have two pairs with opposite spin, each with energy $-\beta_2/4$. Hence, the difference in energy compared to the ground state is $-\beta_2$.

[8] Since the bosons in reality are neutral, this corresponds to fractional particle number in the experimental system.

Chapter 5

The Read-Rezayi states

In the previous chapters we have looked at two different non-abelian systems and illustrated how elementary excitations are formed as domain walls between different ground states on the thin torus, leading to a charge splitting caused by the nontrivial ground state degeneracy. In this chapter this picture will be generalized to a large class of non-abelian systems—the so-called Read-Rezayi (RR) states [39]. The treatment follows parts of Paper II.

5.1 Ground states on the thin torus

The Read-Rezayi states are candidates for describing the FQHE at filling $\nu = \frac{k}{kM+2}$, where $k \geq 1$, $M \geq 0$, and M even (odd) corresponds to bosonic (fermionic) systems. The RR wave functions are ground states of certain local $k+1$-body interactions (c.f. the three-body interaction for the pfaffian MR state) and on the thin torus, because of the suppressed hopping, this interaction forces all clusters of $k+1$ particles to separate. The interaction poses no restriction on how close any k particles may be, but having $k+1$ closely lying particles costs energy. For $M \neq 0$ it also holds that not more than one particle on M consecutive sites are allowed.

It is clear that an even spread in particle density minimizes the energy, because such a configuration keeps *any* clusters of particles, and in particular any clusters of size $k+1$, as separate as possible. These are the, by now well-known, TT states; for $k = 3$, $M = 0$, they are $[12] = |1212...\rangle$ and the translated copy $[21] = |2121...\rangle$. The TT states are, however, not the only to minimize the repulsive $k+1$-body interaction. The only thing one has to bother about is clusters of $k+1$ particles; in this particular case ($k = 3$),

clusters of four particles. The state $[30] = |3030...\rangle$ also keeps any four particles as separate as possible, and has thus the same low energy as [12]. In general, for filling fraction $\nu = \frac{k}{2}$, one finds that the energy is minimized by all states which have exactly k particles on any string of two consecutive sites. These states may be labeled

$$[k-l, l] = |k-l, l, k-l, l, \ldots\rangle, \tag{5.1}$$

where $l = 0, 1, \ldots, k$.

k	M	Unit cells	Degeneracy
1	1	100	3
2	0	11, 20	3
2	1	1010, 1100	6
2	2	100100, 101000	9
3	0	21, 30	4
4	0	22, 31, 40	5

Table 5.1: *A few examples of RR states on the thin torus. Table originally by E.J. Bergholtz.*

As long as N_s is even, every state $[k-l, l]$ fulfills the periodic boundary conditions of the torus. Since there are $k+1$ different values of l, the degeneracy is $k+1$ in this case. However, for N_s odd there is only one possibility, namely the state $[k/2, k/2]$, which only exists when k is even. To summarize: N_s even implies a degeneracy of $k+1$. N_s odd, k even, yields a degeneracy of one. N_s odd, k odd, implies zero degeneracy. For $M \neq 0$, this generalizes to a degeneracy $(k+1)(kM+2)/2$ when $2N_e/k = 0 \bmod 2$, and $(kM+2)/2$ when $2N_e/k = 1 \bmod 2$. A few examples of the RR states on the thin torus are found in Table 5.1.

5.2 Minimal excitations

Now, let us find the minimal excitations for the RR states using the thin-torus approach. The ground states for $M = 0$, minimizing the $k+1$-body interaction, are such that any string of two consecutive sites host exactly k particles. There are N_s such strings, one starting at each site. Clearly,

the least deviation from this pattern, under the influence of the $k+1$-body interaction, is that of a single string hosting $k \pm 1$ particles in a surrounding of strings hosting k particles. An example of this is the state $|1212\underline{11}212\rangle$, $k = 3$, where the underlined string has less charge than all other strings.

In general, we can create this type of excitation by connecting different ground states. Using the compact unit cell notation of the states, the excitation in the example above may be written [12][21]. Note that this notation does not contain any information about the length of the states, nor if the domain wall is of the type $[12][21] = |1212\underline{11}212\rangle$ (quasihole) or $[12][21] = |121\underline{22}1212\rangle$ (quasiparticle). In general, an elementary excitation is constructed by forming a domain wall between states with l differing by one; $[k-l, l][k-l-1, l+1]$, or, $[k-l-1, l+1][k-l, l]$, $0 \leq l < k$.

The formation of domain walls can be pictured in a so-called Bratteli diagram [40] as in Fig. 5.1, here for $k = 4$. Each state, labeled by the integer l, which we also use to label the corresponding "levels", may only be connected to states in the adjacent levels, $l' = l \pm 1$. Each transition between levels creates a quasihole or a quasiparticle.

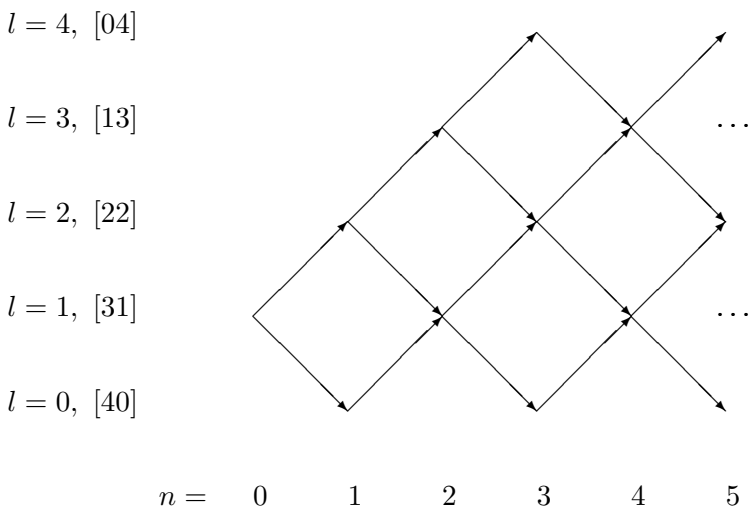

Figure 5.1: *A Bratteli diagram for $k = 4$. The diagram illustrates how fractionally charged domain walls are constructed through transitions between states with $\Delta l = 1$, starting with the state* [31]. *The integer n denotes the number of domain walls. Figure by E.J. Bergholtz.*

The fractional charge of a domain wall is, for general M,

$$e^* = \pm\frac{e}{kM+2}, \tag{5.2}$$

where e is the charge of the particles in the system. This can be explained in the following manner. In the ground state, every string of $kM+2$ consecutive sites host k particles and, thus, the charge ek. In other words, the particle density is $\frac{ek}{kM+2}$ in all N_s strings and the total charge of the ground state is

$$eN_e = N_s\frac{ek}{kM+2}. \tag{5.3}$$

When excitations are added, the charge at each domain wall is $e(k\pm1)$ per $kM+2$ sites and the total charge of the state changes to

$$eN_e = (N_s - n_{qp} - n_{qh})\frac{ek}{kM+2} + n_{qp}\frac{e(k+1)}{kM+2} + n_{qh}\frac{e(k-1)}{kM+2}, \tag{5.4}$$

where n_{qp}, n_{qp} are the number of quasiparticles and quasiholes respectively. We rewrite this equation as

$$eN_e = N_s\frac{ek}{kM+2} + (n_{qp} - n_{qh})\frac{e}{kM+2}, \tag{5.5}$$

by which we readily confirm Eq. (5.2); each quasiparticle or quasihole contributes with $e^* = \pm\frac{e}{kM+2}$ to the total charge of the state.

Chapter 6

Fractional charges in optical lattices

In Section 2.3.1 we introduced the TT states as the q-fold degenerate lattice ground states at $\nu = p/q$ in the thin-torus limit, i.e., in the absence of hopping. Studies suggest that there generically exists a continuous connection between these states and the abelian quantum Hall states that are present on the plane, recreated by increasing the torus circumferences to infinity. As mentioned, this cannot immediately be generalized to non-abelian states. Since these are characterized by a nontrivial increase of the ground state degeneracy that goes beyond the q-fold center-of-mass degeneracy, a phase transition must in those cases separate the infinitely thin torus and the bulk.[1] However, one can make use of the TT limit also in the non-abelian case by adjusting the electrostatic interaction in specific ways. This will be illustrated in this chapter, where we treat another one-dimensional problem, namely optical lattices in one dimension. We will show that for some electrostatic interactions, particle configurations and fractional domain walls corresponding to certain non-abelian QH states can be realized in the optical lattice. The ideas presented here are also found in Paper IV.

[1] In Chapter 3 and 4 we considered two non-abelian systems on the thin, but not infinitely thin, torus—in the regimes where the phase transition to the bulk phase had already taken place.

6.1 Extended Bose-Hubbard model

Consider the extended Bose-Hubbard hamiltonian

$$\hat{H} = \frac{V_0}{2} \sum_i \hat{n}_i(\hat{n}_i - 1) + \sum_i \sum_{j>0} V_j \hat{n}_i \hat{n}_{i+j} - \mu \sum_i \hat{n}_i, \tag{6.1}$$

where V_0 is the energy cost for having a pair of particles on the same site and μ is the chemical potential—a parameter that determines the energy gain ($\mu \geq 0$ is assumed) associated with increasing the number of particles. The chemical potential will determine the filling fraction of the system; the larger μ is, the larger ν becomes. In this sense it has the same effect as the magnetic field strength has for the quantum Hall system, where large B implies small ν.

Among the experimental systems that to fair approximations are captured by Eq. (6.1), one finds tetracyanoquinodimethane (TCNQ) salts [41] as well as atoms or molecules in one-dimensional optical lattices [42, 43]. The latter has the great advantage of being accessible for tuning of interaction parameters, such as hopping, chemical potential and on-site interaction [43, 44]. Obviously, this opens up for realizing different phases in the lattice, depending on the nature of the interaction at hand [45].

It turns out that the values of the second derivatives

$$V_j'' \equiv V_{j-1} + V_{j+1} - 2V_j \tag{6.2}$$

of the discrete set of parameters V_j determine the phase acquired by the system [41]. This can be understood by considering the situation in Fig. 6.1. In the left state in the figure, the particle in the middle has two neighbors at the distance j. In the right state the middle particle has moved one lattice site to the left, resulting in one neighbor at the distance $j-1$, and one at the distance $j+1$. The energy difference between the two states is V_j'', meaning that the sign of V_j'' says whether it is profitable to pair particles (rightmost state) or spread them out (leftmost state). When $V_j'' < 0$, pairing is favored.

Interactions that fulfill $V_j'' > 0$, $V_j \geq 0$, $\forall j \geq 1$, are called *convex interactions*. In this category one finds, e.g., Coulomb, screened Coulomb and dipole-dipole interaction $V_j = V_1/j^3$ (assuming V_0 is large enough). As opposed to this, *non-convex* interactions will in this thesis refer to any set of interaction parameters which do *not* fulfill $V_j'' > 0$, $\forall j \geq 1$. In coming sections we will consider interactions whose non-convexity is defined through $V_j'' = 0$ for some j, while all other $V_j'' > 0$. Let us first, however, discuss convex interactions.

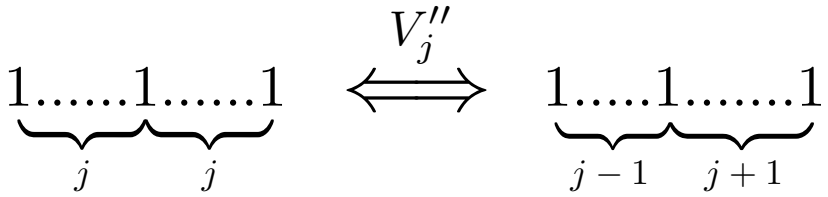

Figure 6.1: *Illustration of the meaning of V_j''; the energy difference between the left and the right state is $V_j'' = V_{j-1} + V_{j+1} - 2V_j$.*

6.2 Convex interactions

The solution for convex interactions is well known since earlier[2] and we have actually already presented the low-energy states emerging in this case—the TT states and their fractionally charged domain wall excitations. From the discussion in Section 6.1 it is clear that whenever $V_j'' = V_{j-1}+V_{j+1}-2V_j > 0$ for all j, a completely even spreading-out of the particles is favored. For bosons, all filling fractions $\nu = p/q \geq 0$ are allowed and examples of ground state unit cells are [100] for $\nu = 1/3$, and [23] for $\nu = 5/2$. Minimal excitations $e^* = \pm e/q$ are formed in the familiar way as domain walls between translated copies of the q-fold degenerate TT states; for $\nu = 5/2$ we have, e.g., [23][32] = $|...232\underline{33}232...\rangle$, where the red-colored and underlined string has charge $e^* = e/2$. Since the gapped ground states appear for each rational filling fraction $\nu = p/q$, the phase diagram can be pictured by a so-called Devil's staircase; if ν is plotted as a function of the chemical potential μ, plateaus emerge whenever ν takes a rational number.

6.3 A particular choice of non-convex interaction

Let us now turn our attention to a specific choice of *non-convex* interaction, defined by $V_0 = 2V_1$ and $V_{j>1} = 0$.[3] This is equivalent to $V_1'' = 0$, $V_2'' > 0$, and $V_{j>2}'' = 0$, which tells us that the particles in the lattice should be subject to some amount of pairing.

[2] See, e.g., [23, 24, 41, 46, 47].

[3] Studies (besides the ones presented in thesis) treating non-convex interactions include [47, 48]. Related numerical studies are described in [49, 50].

For the given values of V_j, the hamiltonian in Eq. (6.1) reduces to

$$\hat{H} = \frac{V_0}{2}\sum_i \hat{n}_i(\hat{n}_i - 1) + \sum_i V_1 \hat{n}_i \hat{n}_{i+1} - \mu \sum_i \hat{n}_i = \\ = \sum_i \frac{V_0}{2}\Big(\hat{n}_i(\hat{n}_i - 1) + \hat{n}_i\hat{n}_{i+1}\Big) - \mu\hat{n}_i. \tag{6.3}$$

Clearly, each particle added to the system *decreases* the energy by μ, but every pair of nearest neighbors *increases* the energy by $V_0/2$, just as every pair of on-site neighbors increases it by V_0. In minimizing the total energy, the system has to walk a tightrope while adding as many particles as possible and yet avoiding too many on-site or nearest-neighbor pairs. The larger μ is, the more interacting particle pairs can be afforded. The question is, which phases are actually realized, depending on the value of μ?

6.3.1 Nontrivially degenerate lattice ground states

We first conclude that we are not charged anything in terms of electrostatic energy for filling the system with particles up to $\nu = 1/2$, because up to this point we can occupy sites without having to deal with any on-site or even nearest-neighbor interactions, simply by forming the TT state [10]. Hence, for any positive μ, the total energy will obviously decrease for every extra particle added up to, at least, filling one-half.

Secondly, when $\nu = 1/2$ has been reached, every particle added beyond this will inadvertently lead to the formation of on-site or nearest-neighbor pairs. In other words, raising the number of particles is no longer free of charge from an electrostatic perspective. It can be realized that each particle added to the half-filled state gives rise to—at least—either two nearest-neighbor pairs, or one on-site pair, both of which equals an energy cost V_0. These minimal changes are implemented by occupying the available empty sites by single particles or by increasing the particle number on the already occupied sites in [10] like $n_i = 1 \to n_i = 2$. Since these processes correspond to minimal increases in electrostatic energy, the TT state [10] remains the ground state as long as $0 < \mu < V_0$. However, when $\mu > V_0$, the minimal increase V_0 in electrostatic energy is compensated for by the chemical potential and it becomes profitable to add particles to the system again—at least as long as this can be done at the cost of V_0, which happens to be the case up to filling $\nu = 1$. Then, either every empty site has been filled, or every site originally hosting one particle now hosts two, and the ground

states are the TT state [11], and the state [20].[4] The reader recognizes these as the thin-torus limits of the Read-Rezayi states at $k = 2$, $M = 0$, see Chapter 5.

Having reached $\nu = 1$ it is no longer possible to add particles at the cost V_0; the minimum fee is instead $2V_0$ and the lattice states [11], and [20], remain the ground states for $V_0 < \mu < 2V_0$. As μ exceeds $2V_0$, particles may be added to every second site in the $\nu = 1$ ground states [11] or [20] (at the electrostatic cost $2V_0$) until the states [21] or [30] are reached at $\nu = 3/2$.

The pattern continues to repeat as μ increases and for $(k-1)V_0 < \mu < kV_0$, $k \in \mathbb{N}^+$, the ground states of Eq. (6.3) are all states with periodicity two at filling fraction $\nu = k/2$, i.e., the states with unit cells $[l, k-l]$, $l = 0, 1, \ldots, k$. Again, the reader recognizes these as the thin-limit versions of the RR states for $M = 0$. Constructing the phase diagram as a function of μ, plateaus of width V_0 appear at every $\nu = k/2$, see Fig. 6.2. At the intermediate points $\mu = kV_0$, all fillings $k/2 \leq \nu \leq (k+1)/2$ are represented.

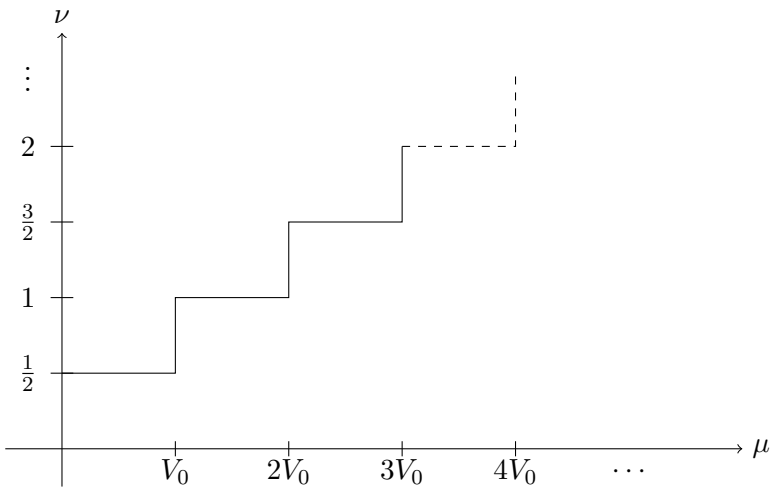

Figure 6.2: *Phase diagram of Eq. (6.3) as a function of the chemical potential μ. Within each plateau, every state with periodicity two at the given filling fraction $\nu = k/2$ belongs to the ground state manifold. Figure by T. Kvorning.*

[4] Center-of-mass translations are implicitly included.

6.3.2 Fractional excitations

Let us find the smallest excitation that can be created in the lattice system within the plateau $(k-1)V_0 < \mu < kV_0$. The minimum electrostatic cost for simply adding a particle to filling $\nu = k/2$ is, according to Section 6.3.1, kV_0. This is compensated for, to a larger or smaller extent, by the chemical potential, which decreases the energy by μ. The minimum net excitation energy for adding a particle is, thus, $\Delta E = kV_0 - \mu$, with $(k-1)V_0 < \mu < kV_0$. Analogously, a particle can be removed from one of the ground states at the expense of $\Delta E = \mu - (k-1)V_0$, $(k-1)V_0 < \mu < kV_0$. Depending on the value of μ, these energy costs range between $0 < \Delta E < V_0$. However, excitations involving reorganization of particles are also available for the system and the general minimal excitations are fractionally charged domain walls between $[l, k-l]$ and $[l \pm 1, k-l \mp 1]$, as explained in Chapter 5.

A process which does not involve an increase or decrease of the filling fraction is the construction of a particle-hole excitation. The cost of inserting a string of one ground state into the other so that one $+e/2$-charge and one $-e/2$-charge are created is $\Delta E = V_0/2$, independent of k and μ. Like before, domain walls of alike sign can also be formed, so that the resulting filling fraction is either larger or smaller than in the unperturbed ground state. Forming two quasiparticle domain walls of charge $+e/2$ each adds one extra particle to the system and has an excitation energy $\Delta E = kV_0 - \mu$, equal to the cost of adding one charge $+e$ to a specific site. Analogously, the excitation energy for a pair of quasiholes is $\Delta E = \mu - (k-1)V_0$. This is a consequence of the short-range interaction; the distance between the domain walls is irrelevant and the single particle added to one of the sites may be viewed as two fractionally charged domain walls on top of each other.

In analogy to what is stated in Chapter 5, the domain walls have the property that there are several inequivalent ways to produce an excitation at a given position on the lattice. Again, this feature is suited for the construction of a Bratteli diagram [40], which in Fig. 6.3 is presented along with a sketch showing how two different paths in the Bratteli diagram translate into particle numbers at different sites in the optical lattice.

6.3.3 Experimental relevance

The hamiltonian in Eq. (6.3) has been chosen to select the periodic states $[l, k-l]$ and their fractionally charged excitations. The optical lattice setting is such that the on-site parameter V_0 can be tuned to ensure $V_1'' = 0$ [43]. However, the requirement $V_{j>1=0}$ is somewhat artificial and a more realistic

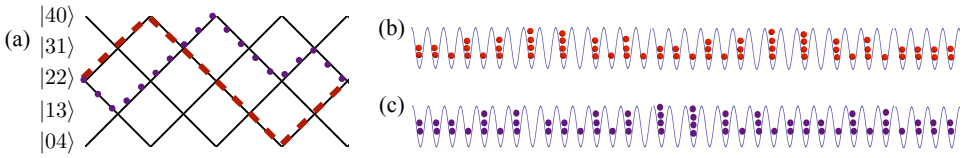

Figure 6.3: *The Bratteli diagram for $\nu = k/2 = 2$ is seen in (a). The state in (b) shows a possible particle configuration corresponding to the dashed, red line and a possible configuration corresponding to the purple, dotted line is shown in (c). Figure by E.J. Bergholtz, borrowed from Paper IV.*

electrostatic interaction from an experimental point of view is the dipole-dipole potential $V_j = V_1/j^3$ [51]. Important for the creation of domain wall excitations is the degeneracy of the states $[l, k-l]$ for different values of l. To investigate if this degeneracy can be achieved also for the dipole-dipole interaction, we first note that the energy difference between the wanted states is proportional to $\sum_{j\geq 1} V''_{2j-1}$. Thus, to make them degenerate, one needs to ensure that this sum is zero, which for the dipole-dipole potential means

$$\begin{aligned} 0 &= \sum_{j\geq 1} V''_{2j-1} = V_0 + 2V_1 \sum_{j\geq 1} \frac{(-1)^j}{j^3} = V_0 - V_1 \frac{3}{2}\zeta(3) \\ &\approx V_0 - 2V_1 \times 0.9015, \end{aligned} \tag{6.4}$$

where $\zeta(x)$ is the Riemann ζ function. Note that this imposes only a minor shift from the previous requirement $V_0 = 2V_1$. When fulfilling this, the excitation structure in terms of fractional domain walls will remain qualitatively the same. However, whereas the distance between the domain walls did not matter for the short-range interaction, the long-range dipolar interaction will lead to a tendency for domain walls of equal sign to repel.

Another issue is the effect of non-zero hopping in the optical lattice. Since the potential wells that confine the particles at the sites are finite in depth, tunneling amplitudes are never zero, although they can be made very small by increasing the laser intensity. In Paper IV this problem is addressed through a perturbative calculation and a numerical analysis. The study suggests that even in the presence of inter-site tunneling, the states $[k, k-l]$ presented here can be made approximately degenerate and that within certain regimes, the fractional excitations should be within the reach of construction—e.g., by varying the chemical potential locally to produce variations in the particle density [52], as illustrated in Fig. 6.4.

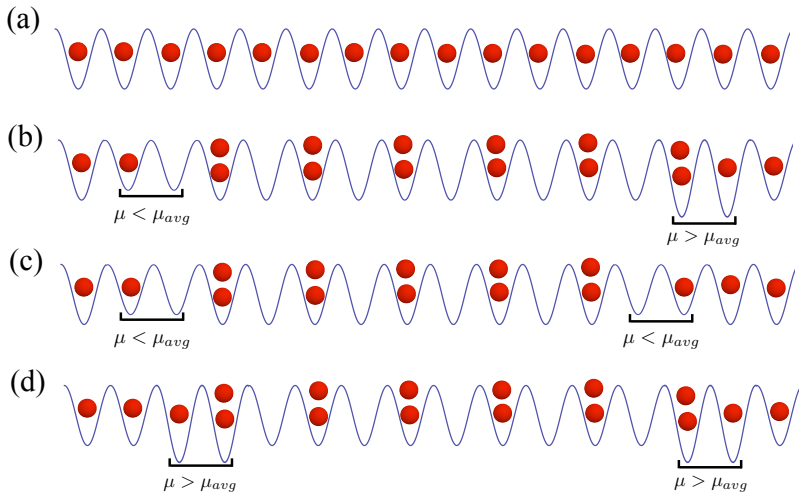

Figure 6.4: *Illustration of how fractional domain walls may form due to local changes in the chemical potential. Here, the chemical potential is varied on two neighboring sites to create the domain walls in (b)–(d) with charge* $e^* = \pm e/2$*, starting from the background state (a). Figure by E.J. Bergholtz, borrowed from Paper IV.*

Chapter 7

Generalized charge splitting and nontrivial degeneracies

Through the previous chapters we have considered both fermionic and bosonic systems using one-dimensional lattice models where hopping or tunneling is ignored and changes in the filling fraction and/or the electrostatic interaction lead to different types of low-energy states. In this chapter we extend these findings by introducing sets of $q(2^m-1)$-fold degenerate ground states and (split) fractional charges of size $e^* = e/mq$, m integer. Here, $m = 0$ corresponds to a convex interaction and gives the ordinary q-fold degenerate TT ground states and fractional charges $e^* = e/q$. Furthermore, $m > 0$ corresponds to certain non-convex interactions and means a nontrivial increase of the ground state degeneracy, which is characteristic for non-abelian systems. In the analysis, on which more details are found in Paper V, we employ a mapping of low-energy states onto spin-1/2 chains. In spin representation, the fractional charges are characterized by domain walls between degenerate ground states where single pairs of mth nearest-neighbor spins have opposite signs. The construction of domain wall excitations are pictured in a Bratteli diagram, and at the end of this chapter we discuss the outlooks of realizing these states in a physical setting.

7.1 Convexity and charge fractionalization revisited

Consider the hamiltonian

$$\hat{H} = \frac{V_0}{2} \sum_i \hat{n}_i(\hat{n}_i - 1) + \sum_i \sum_{j>0} V_j \hat{n}_i \hat{n}_{i+j}. \tag{7.1}$$

This equation can be used to describe any electrostatic interaction between bosons as well as fermions in the one-dimensional lattice, adding the obvious constraint that n_i is restricted to zero or one for fermions. If we assume the filling fraction ν to be adjustable by either tuning a magnetic field or a chemical potential, it captures both the thin-torus limit of the fractional quantum Hall system, and the optical lattices treated in Chapter 6.

As mentioned in Section 6.2, the second derivates $V_j'' = V_{j-1} + V_{j+1} - 2V_j$ of the interaction parameters are crucial for which phase is realized in this system. Convex interactions, fulfilling $V_j'' > 0 \ \forall j \geq 1$, produce the q-fold degenerate TT ground states at filling $\nu = p/q$ and the lowest excitations are fractional charges $e^* = \pm e/q$, being domain walls between mutually translated ground states [21, 24]. However, not all combinations of TT ground states are allowed! The domain walls have to be such that a single string of q consecutive sites hosts no more and no less than $p \pm 1$ particles. This fact poses constraints on how to combine translated copies of the TT state according to the below.

The unit cell of any TT state at $0 < \nu < 1$ can be written $[\tilde{C}10]$, where $\tilde{C}$ is a binary string of length $q-2$, mirror symmetric around its center [53].[1] Also, by moving the rightmost particle one step to the right, a translated copy $[\tilde{C}01]$ of the TT cell is created. In this chapter we will several times use $\nu = 2/5$ to illustrate the ideas; for this specific filling, $\tilde{C} = 010$, which defines the unit cell $[\tilde{C}10] = [01010]$ and the translated version $[\tilde{C}01] = [01001]$. Note that, because of the q-fold degeneracy of the TT state, there are q possible ways to define the "starting point" of the lattice so that $[\tilde{C}10]$ here may represent any of the translated copies.

Now, the nature of a fractional charge $e^* = \pm e/q$ will, due to the requirement of a single string of $p \pm 1$ particles on q sites, always be a domain wall between states represented by $[\tilde{C}10]$, and $[\tilde{C}01]$, respectively. The domain wall $[\tilde{C}10][\tilde{C}01]$ has a *decrease* in the particle density and, thus, corresponds

[1] Fillings $\nu \geq 1$ work much in the same way as long as the on-site interaction V_0 is so large that the integer part of the filling lies as an inert background on the lattice.

to a quasihole, whereas $[\tilde{C}01][\tilde{C}10]$ has an *increased* particle density and corresponds to a quasiparticle. In the state

$$[\tilde{C}01][\tilde{C}10] = |...\tilde{C}01\tilde{C}01\tilde{C}01\underline{\tilde{C}1}0\tilde{C}10\tilde{C}10...\rangle,$$

the marked sequence is the only string of length q hosting $p+1$ particles. All other strings of length q host p particles.

For the purpose of future simplicity, let us introduce the short-hand notation $\tilde{C}10 \equiv \uparrow$, and $\tilde{C}01 \equiv \downarrow$.[2] In this spin-1/2 notation, both of the spin-polarized states $|\uparrow\uparrow\uparrow...\rangle \equiv [\uparrow]$ and $|\downarrow\downarrow\downarrow...\rangle \equiv [\downarrow]$ are copies of the TT state. Here, we have identified the states by their spin unit cells, written within square brackets.

In spin notation, the elementary excitations are simply domain walls between spin-polarized regions; using $\nu = 2/5$ to illustrate this, we consider the domain wall

$$[\downarrow][\uparrow] = [\tilde{C}01][\tilde{C}10] = [01001][01010] = |...0100101001\underline{01010}01010...\rangle.$$

Here, the red-colored and underlined string has charge $e^* = e/5$.

7.2 Non-convexity and generalized charge fractionalization

In Section 5.2 we saw the following. At filling $\nu = \frac{k}{kM+2}$, a single string of length $kM+2$ hosting $k\pm1$ particles has fractional charge $e^* = \pm\frac{e}{kM+2}$. This statement is naturally generalized to filling fraction $\nu = p/q$; a single string of length mq, m integer, hosting $mp\pm1$ instead of mp particles, has fractional charge $e^* = \pm e/mq$. Here, $m = 1$ corresponds to the ordinary construction of $\pm e/q$ charges described in Section 7.1, while $m > 1$ implies an increased charge splitting that can be found in, e.g., non-abelian quantum Hall states. One example of the latter are the Moore-Read states at $\nu = 5/2$, where we have seen domain wall excitations of the kind $|...1010\underline{1011}001100...\rangle$. For the MR excitations, $m = 2$, giving $e^* = \pm e/4$.

To achieve split charges, a nontrivial ground state degeneracy at the filling fraction in question is necessary. In what follows we describe how these ground states can be chosen and how they may combine to form the split excitations.

[2] Note that this is much in the spirit of Section 2.4, where $p = 1$ and $q = 2$, so that $\tilde{C}$ has zero extension and $\tilde{C}10 = 10 \equiv \uparrow$, $\tilde{C}01 = 01 \equiv \downarrow$.

7.2.1 Split fractional charges

In Section 7.1 we saw that an elementary charge $e^* = \pm e/q$ is a domain wall between the TT states $[\tilde{C}10]$ and $[\tilde{C}01]$, because such a domain wall has $p \pm 1$ particles on a single string of q consecutive sites. In spin notation, the domain wall is between the spin-polarized states $[\uparrow]$, and $[\downarrow]$, which offers an equivalent way to describe the fractional excitation: *a fractional charge $e^* = \pm e/q$ is characterized by a single nearest-neighbor pair of opposite spins in a surrounding of nearest-neighbor pairs of equal spins.* The two possibilities are $[\downarrow][\uparrow] = |...\downarrow\downarrow\underline{\downarrow\uparrow}\uparrow\uparrow...\rangle$, and $[\uparrow][\downarrow] = |...\uparrow\uparrow\underline{\uparrow\downarrow}\downarrow\downarrow...\rangle$, where we have colored and underlined the nearest-neighbor spin pair of opposite sign in each state. The first example is a quasihole, while the latter is a quasiparticle.

There is a simple generalization of this rule, corresponding to a nontrivial splitting of the fractional charge $e^* = \pm e/q$, which reads as follows. *A fractional charge $e^* = \pm e/mq$, m integer, is characterized by a single mth nearest-neighbor pair of opposite spins in a surrounding of mth nearest-neighbor pairs of equal spins.* This type of domain wall can in turn be created by combining spin states of periodicity m, which are related by the flipping of one spin in their spin unit cells. For example, the states represented by $[\uparrow\downarrow\downarrow]$ and $[\uparrow\uparrow\downarrow]$, respectively, may be combined to form $\pm e/3q$ charges. In the state

$$[\uparrow\downarrow\downarrow][\uparrow\uparrow\downarrow] = |...\uparrow\downarrow\downarrow\uparrow\underline{\downarrow}\downarrow\uparrow\underline{\uparrow}\downarrow\uparrow\uparrow\downarrow...\rangle,$$

the third-nearest-neighbor pair of opposite spins is red-colored and underlined. Note the rule that the combined spin states must be related by the flipping of one spin in the unit cell; the state $[\uparrow\downarrow\downarrow]$, e.g., may *not* be combined with $[\downarrow\uparrow\uparrow]$, since they are not related by this rule.

The reason why this kind of domain wall corresponds to a fractional charge $e^* = \pm e/mq$ is that the excited state contains a single string of $mp \pm 1$ particles on mq sites, whereas all other strings of the same length host mp particles. This can easily be understood by considering the domain wall in number representation through $\uparrow \rightarrow \tilde{C}10$, $\downarrow \rightarrow \tilde{C}01$. An example, given for $m = 2$, is the state

$$[\downarrow\downarrow][\uparrow\downarrow] = [\tilde{C}01\tilde{C}01][\tilde{C}10\tilde{C}01] = |...\tilde{C}01\tilde{C}01\underline{\tilde{C}01\tilde{C}1}0\tilde{C}01\tilde{C}10...\rangle,$$

where the marked sequence is the only string of length $2q$ to host $2p + 1$ particles.

To make the domain wall construction clearer, let us return to the illustrative example $\nu = 2/5$, $m = 2$, considering the states $[\uparrow\uparrow] = [0101001010]$, $[\uparrow\downarrow] = [0101001001]$, $[\downarrow\uparrow] = [0100101010]$, and $[\downarrow\downarrow] = [0100101001]$. One possible way to create a fractional excitation is to combine $[\downarrow\downarrow] = [0100101001]$ and $[\downarrow\uparrow] = [0100101010]$, constructing

$$[\downarrow\downarrow][\downarrow\uparrow] = |...\downarrow\downarrow\underline{\downarrow}\downarrow\underline{\uparrow}\downarrow\uparrow\downarrow...\rangle = |...0100\underline{10100101010}01001...\rangle.$$

Here, the next-nearest-neighbor pair of opposite spins and the corresponding fractionally charged ($e^* = e/10$) string are colored and underlined.

7.2.2 Nontrivially degenerate ground states

For the construction of split fractional charges $e^* = \pm e/mq$, we are interested in states with spin unit cells of length m (in number representation, unit cells of length mq), consisting of m copies of $\uparrow = \tilde{C}10$ and/or $\downarrow = \tilde{C}01$ in any order. For $m = 3$, e.g., the states are $[\uparrow\uparrow\uparrow]$, $[\uparrow\uparrow\downarrow]$, $[\uparrow\downarrow\uparrow]$, $[\downarrow\uparrow\uparrow]$, $[\uparrow\downarrow\downarrow]$, $[\downarrow\uparrow\downarrow]$, $[\downarrow\downarrow\uparrow]$ and $[\downarrow\downarrow\downarrow]$.[3] As we have seen, what is interesting and special about these states is that they, combined in the right way, can be used to construct fractional charges $e^* = \pm e/mq$. Let us formalize the treatment of the states by introducing a new notation.

Let $S_{m,j}$, $j = 0, 1, ..., m$, be the set of spin states whose unit cells of length m consist of j spin-downs and $(m-j)$ spin-ups in any order. The fractionally charged domain walls are between states in $S_{m,j}$, and *appropriate* states in $S_{m,j\pm1}$; as we have seen, when creating $\pm e/3q$ charges, the state $[\uparrow\downarrow\downarrow]$ in $S_{3,2}$ may be combined with $[\uparrow\uparrow\downarrow]$ in $S_{3,1}$, but not with $[\downarrow\uparrow\uparrow]$, since the two are not related by the flipping of one single spin. Clearly, each state in $S_{m,j}$ may be combined with j different states in $S_{m,j-1}$ and $m - j$ states in $S_{m,j+1}$. Note that the domain wall $[S_{m,j}][S_{m,j-1}]$ corresponds to a fractional charge $e^* = +\frac{e}{mq}$, whereas $[S_{m,j}][S_{m,j+1}]$ corresponds to a charge $e^* = -\frac{e}{mq}$.

Obviously, there are $\binom{m}{j}$ different spin states within the set $S_{m,j}$. Summing over $j = 0, 1, ..., m$, the total number of spin states becomes $\sum_{j=0}^{m}\binom{m}{j} = 2^m$. To count how many lattice states, expressed in number representation, this corresponds to, remember that there are q translations of the TT state, each of which can be identified as $\tilde{C}10 = \uparrow$. In other words, there are effectively q copies of the spin space, which makes it tempting to identify $2^m q$ as the total degeneracy. However, each TT state appears in two different

[3] Please note that the spin-polarized TT states, together with some other states, such as $[\uparrow\downarrow\uparrow\downarrow]$ ($m = 4$), have reducible unit cells.

spin space copies—in one in the shape of $[\uparrow\uparrow ... \uparrow]$, and in one in the shape of $[\downarrow\downarrow ... \downarrow]$. Hence, the degeneracy is

$$d_{q,m} = q \sum_{j=1}^{m} \binom{m}{j} = q(2^m - 1), \tag{7.2}$$

where $j = 0$ has been excluded to avoid double-counting of the TT states. Note that Eq. (7.2) reproduces the ordinary q-fold center-of-mass degeneracy for $m = 1$; in this case we search for states with spin unit cells of length one, which is satisfied only by the TT states $[\uparrow]$ and $[\downarrow]$. On the other hand, $m > 1$ implies an increased degeneracy, where the TT state is joined by other, translationally inequivalent, lattice states.

As an illustration, let us consider $\nu = 2/5$, $m = 2$. Here, the states can be divided into five copies of the spin subspace[4];

$$\begin{aligned}
&S^{(1)}_{2,0} = \{[\uparrow\uparrow] = [0101001010]\},\\
&S^{(1)}_{2,1} = \{[\uparrow\downarrow] = [0101001001], [\downarrow\uparrow] = [0100101010]\},\\
&S^{(1)}_{2,2} = \{[\downarrow\downarrow] = [0100101001]\},
\end{aligned}$$

$$\begin{aligned}
&S^{(2)}_{2,0} = \{[0100101001]\} = S^{(1)}_{2,2},\\
&S^{(2)}_{2,1} = \{[0100100101], [0010101001]\},\\
&S^{(2)}_{2,2} = \{[0010100101]\},
\end{aligned}$$

$$\begin{aligned}
&S^{(3)}_{2,0} = \{[0010100101]\} = S^{(2)}_{2,2},\\
&S^{(3)}_{2,1} = \{[0010010101], [1010100100]\},\\
&S^{(3)}_{2,2} = \{[1010010100]\},
\end{aligned}$$

$$\begin{aligned}
&S^{(4)}_{2,0} = \{[1010010100]\} = S^{(3)}_{2,2},\\
&S^{(4)}_{2,1} = \{[1010010010], [1001010100]\},\\
&S^{(4)}_{2,2} = \{[1001010010]\},
\end{aligned}$$

and

[4]The ordering of the spin subspaces is chosen so that $\left[S^{(i)}_{m,m}\right] = \left[S^{(i+1)}_{m,0}\right]$.

$$S^{(5)}_{2,0} = \{[1001010010]\} = S^{(4)}_{2,2},$$
$$S^{(5)}_{2,1} = \{[1001001010],\, [0101010010]\},$$
$$S^{(5)}_{2,2} = \{[0101001010]\} = S^{(1)}_{2,0}.$$

From this list, we identify the inequivalent unit cells $[0101001010] \equiv [01010]$ (TT state, five translations) and [0101001001] (ten translations), which means a degeneracy in agreement with $d_{5,2} = 5(2^2 - 1) = 15$.

Now, let us return to the construction of domain walls. Note that if sequences of more than $q-1$ consecutive quasiparticles (or, analogously, quasiholes) are to be created, states from several copies of the spin subspace need to be included. This problem is resolved by noticing that the TT state $\left[S^{(i)}_{m,m}\right]$ in one subspace equals $\left[S^{(i+1)}_{m,0}\right]$ in another subspace, which, e.g., implies that $\left[S^{(i)}_{m,0}\right]\left[S^{(i+1)}_{m,m-1}\right] = \left[S^{(i+1)}_{m,m}\right]\left[S^{(i+1)}_{m,m-1}\right]$ corresponds to a quasiparticle. An example of a state with six quasi-holes, here for $m = 3$, is

$$\left[S^{(i)}_{3,0}\right]\left[S^{(i)}_{3,1}\right]\left[S^{(i)}_{3,2}\right]\left[S^{(i+1)}_{3,0}\right]\left[S^{(i+1)}_{3,1}\right]\left[S^{(i+1)}_{3,2}\right]\left[S^{(i+2)}_{3,0}\right].$$

Like in Section 5.2, a Bratteli diagram gives a nice overview of the domain wall construction. In Fig. 7.1, a quasihole is created in each downward step and each step upwards creates a quasiparticle. Here, each level of states, denoted $\left[S^{(i)}_{m,j}\right]$, represents all $\binom{m}{j}$ different states contained in the set $S^{(i)}_{m,j}$.

7.2.3 Interaction tuning and experimental prospects

Up to this point we have postponed a very important question. We have described how split fractional charges emerge as domain walls between certain lattice states, represented by spin states of periodicity m. However, for the charges $e^* = \pm\frac{e}{mq}$ to be realized in a physical setting, interaction parameters need to be adjusted so that these states become degenerate ground states. We need to address whether they even *can* be degenerate ground states for *any* choice of interaction! In this section we wish to discuss the outlooks for the emergence of the described low-energy states in the laboratory, as well as to shed light on interesting connections to known physical systems.

The values of the interaction parameters V_j'' determine the phase of the one-dimensional lattice system, see Section 6.2. When all $V_j'' > 0$, i.e., whenever the interaction is convex, the TT states and their elementary excitations of charge $\pm e/q$ constitute the low-energy sector. However, by shrinking one or several V_j'' to zero, other states can join the TT states in

the ground state manifold and produce the nontrivial degeneracy that is characteristic for non-abelian systems. (We assume $V_j'' \geq 0$.)

It turns out[5] that an interaction which lets $V_{kq}'' = 0$, k integer, with the exception $V_{mq}'' > 0$, produces the spin states of periodicity m. In fact, other parameters $V_{j\neq kq}''$ may also be shrunk to zero, as long as $V_{j<q}'' > 0$. The Moore-Read state [28], treated in Chapter 3, serves as a simple example.

The MR state supports fractional charges $e^* = \pm e/4$, and in the thin-torus limit the sixfold degenerate ground states are of the types $[1010] = [\uparrow\uparrow]$, and $[1001] = [\uparrow\downarrow]$. Since $q = 2$ and $e^* = \pm e/4$, this case corresponds to $m = 2$, which means that one should choose an interaction such that $V_{2k}'' = 0$, $k \neq 2$, and $V_4'' > 0$. Due to the requirement $V_{j<q}'' > 0$, $V_1'' > 0$ has to be assumed as well. Under these circumstances, the MR states and their fractional excitations are the low-energy states of the lattice system. Note that this conclusion agrees with the analysis in Section 3.1.

Another issue that needs to be addressed at this point is the problem of fine-tuning. It seems here, that in order to achieve the exotic states and excitations given by $m > 1$, the interaction parameters need to be fine-tuned in a way that speaks against those states being of physical relevance. Although the techniques used in optical lattices allow for tuning of the on-site interaction V_0 [44]—and, thus, V_1''—the like is currently not possible for other individual V_j''. However, we note that some of the states described in this chapter correspond to already known abelian, and non-abelian, quantum Hall states, which are of high experimental relevance and do not require fine-tuning to exist. These states may all be pictured as being the unique ground states of effective repulsive many-body interactions, analogous to the $k+1$-body interaction relevant for the Read-Rezayi states for $M = 0$. Preliminary investigations indicate that this might be possible to generalize to several other states presented in this study. In all cases we have considered so far, the nontrivially degenerate states contained in the spin subspace are ground states of certain choices of repulsive many-body interactions. For example, the states at $\nu = 2/5$, $m = 2$, i.e., the states of type $[\uparrow\uparrow] = [0101001010]$, and $[\uparrow\downarrow] = [0101001001]$, are produced by a five-body interaction allowing no more than four particles on ten consecutive sites, together with a four-body interaction allowing no more than three particles on seven consecutive sites, and a two-body interaction allowing no more than one particle on two consecutive sites. These results make it interesting to investigate whether these and other lattice states not mentioned here could actually correspond to physical states as well.

[5] See the appendix in Paper V.

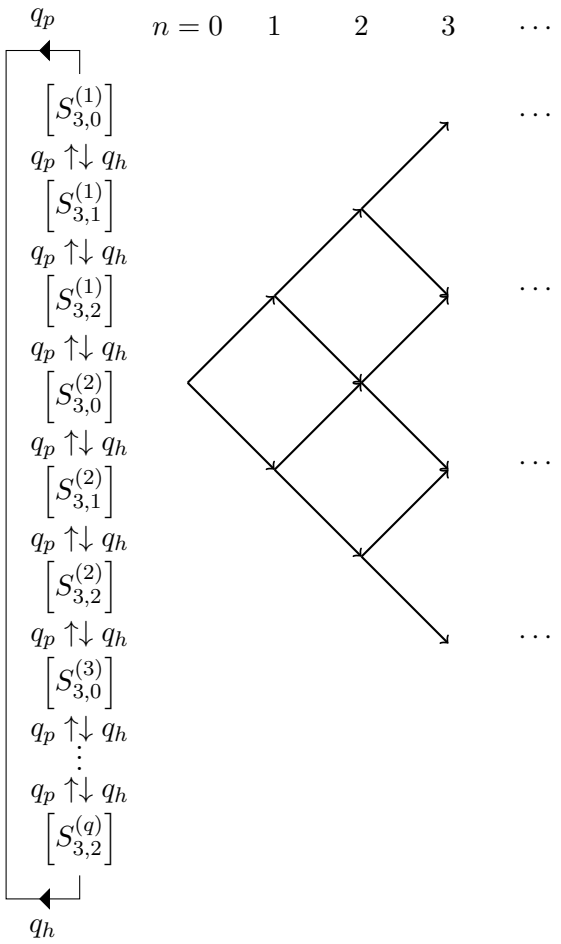

Figure 7.1: *Formation of domain walls between different spin states, $m = 3$. Going from left to right, an excitation is created in each step; n denotes the number of domain walls. In this particular example, the various ways to create excitations starting from a state in $S^{(2)}_{3,0}$ are illustrated. Each "clockwise" step creates a quasihole ($e^* = -\frac{e}{mq}$), whereas every "anti-clockwise" step creates a quasiparticle ($e^* = \frac{e}{mq}$), as indicated by the arrows between different levels. Figure by T. Kvorning.*

Chapter 8

Summary

We have studied a number of systems—bosonic and fermionic—using one-dimensional lattice models that, in their simplicity, show to be highly relevant for describing interesting physical properties. The main example is the fractional quantum Hall system, which, though two-dimensional in the laboratory, can be treated as one-dimensional when mapped onto the torus geometry. In the limit where the torus circumference becomes thin, hopping terms in the hamiltonian diminish, a fact that greatly simplifies the problem of finding ground states and low-energy excitations. Another system that allows for a similar treatment is particles trapped in a one-dimensional optical lattice. There, interaction parameters are to a high extent adjustable, which offers possibilities to tune the system through various phases.

In the one-dimensional lattice, when hopping or tunneling is ignored, the energy states are crystalline-like states with the constituting particles fixed at specific lattice sites. Minimal excitations are generically formed as domain walls between degenerate such ground states. In the abelian case, the degeneracy originates from trivial center-of-mass translations of the lattice states, while the non-abelian ditto requires a nontrivial degeneracy of states not related by translation. The domain walls carry fractional charge (or, fractional particle number for neutral particles), which undergoes extra splitting in non-abelian systems.

In several of the cases treated in this thesis, the analysis has been aided by mapping the low-energy states on the thin torus onto one-dimensional spin chains. Depending on the filling fraction ν and the interaction at hand, different terms in the resulting spin hamiltonian dominate, giving a microscopic understanding of the acquired phases. For example, for fermions at filling $\nu = 1/2$ in the quantum Hall system, the truncated hamiltonian is

dominated by the nearest-neighbor spin flip, yielding a description of this gapless state in terms of neutral dipoles (this was earlier found in [25]).

Chapter 3 in this thesis was dedicated to comparing the two half-filled quantum Hall systems $\nu = 1/2$, and the Moore-Read (MR) state $\nu = 5/2$, which display very different behavior in the laboratory; while the first is gapless and lack fractional charges, the latter is a presumably non-abelian system with charge carriers $e^* = \pm e/4$. We applied the thin-torus description together with the same spin chain mapping used for $\nu = 1/2$. At half-filling in the second Landau level, a negative next-nearest neighbor Ising term produces sixfold degenerate ground states of the type $|1100...\rangle$, and $|1010...\rangle$. Also, it yields gapped, fractionally charged excitations $e^* = \pm e/4$, emerging as domain walls between different ground states. This is all in agreement with what is expected from the MR wave function.

Similar results were presented in Chapter 4, treating the bosonic system $\nu = 1$. In this case (employing a slightly different spin mapping), the next-nearest-neighbor Ising term generates the threefold degenerate ground states $|1111...\rangle$, $|2020...\rangle$, and $|0202...\rangle$, as well as fractional charges $e^* = \pm e/2$. Again, this is in agreement with the properties of the bosonic Moore-Read wave function that is believed to describe this system.

The domain wall picture was generalized in Chapter 5, in a treatment of the so-called Read-Rezayi (RR) states at filling fraction $\nu = \frac{k}{kM+2}$. These states are known to be ground states of repulsive $k+1$-body interactions, which on the thin torus manifest in crystalline states where any string of $kM+2$ sites is occupied by exactly k particles. The fractional charges are $e^* = \pm\frac{e}{kM+2}$ and the construction of the nontrivially degenerate domain walls is advantageously illustrated in so-called Bratteli diagrams.

In Chapter 6 we considered an extended Bose-Hubbard model, primarily relevant for particles in one-dimensional optical lattices. We presented sets of lattice states which—for relatively weak on-site repulsion and suppressed tunneling amplitudes—display low-energy excitations in the form of fractionally charged domain walls, in similarity to the ones found in fractional quantum Hall systems (to be specific, the RR states for $M = 0$). The possibility to tune interaction parameters in optical lattices offers hope that these nontrivially degenerate states, as well as their domain wall excitations, can be studied experimentally in a very controllable setting.

Finally, Chapter 7 treated another one-dimensional lattice hamiltonian, relevant for both the quantum Hall system and optical lattices. There, we generalized the fractional domain wall construction through the nontrivial degeneracy of certain lattice states, by which fractional excitations of charge $e^* = \pm\frac{e}{mq}$, m integer, emerged. The ordinary quantum Hall charges $e^* = \pm\frac{e}{q}$

and the corresponding lattice states are given by $m = 1$. The investigation involves a fine-tuning of the interaction parameters. However, the fact that the study reproduces several physical states that clearly are not relying on fine-tuning for their existence (they are stable against perturbations), indicates that this can hold also for other states included in the model. This suggestion is supported by preliminary investigations in which the fine-tuned interaction parameters are replaced by repulsive many-body interactions like the ones generating the RR states.

Bibliography

[1] E.H. Hall, Journal of Mathematics **2**, 287 (1879).

[2] K.v. Klitzing, G. Dorda and M. Pepper, Phys. Rev. Lett. **45**, 494 (1980).

[3] D.C. Tsui, H.L. Stormer and A.C. Gossard, Phys. Rev. Lett. **48**, 1559 (1982).

[4] K.S. Novoselov, Z. Jiang, Y. Zhang, S.V. Morozov, H.L. Stormer, U. Zeitler, J.C. Maan, G.S. Boebinger, P. Kim, and A.K. Geim, Science **315**, 1379 (2007).

[5] R.L. Willett, J.P. Eisenstein, H.L. Störmer, D.C. Tsui, A.C. Gossard and J.H. English, Phys. Rev. Lett. **59**, 1776 (1987).

[6] S.M. Girvin, *Topological Aspects of Low Dimensional Systems* (Springer-Verlag, Berlin and Les Editions de Physique, Les Ulis, 2000).

[7] L.D. Landau and E.M. Lifshitz, *Quantum Mechanics* (Pergamon Press, New York, 1994).

[8] R.B. Laughlin, Phys. Rev. Lett. **50**, 1395 (1983).

[9] F.D.M. Haldane, Phys. Rev. Lett. **51**, 605 (1983).

[10] B.I. Halperin, Phys. Rev. Lett. **52**, 1583, 2390(E) (1984).

[11] V.J. Goldman, and B. Su, Science **267**, 1010 (1995).

[12] R. de-Picciotto, M. Reznikov, M. Heiblum, V. Umansky, G. Bunin, and D. Mahalu, Nature **389**, 162 (1997).

[13] J.M. Leinaas, and J. Myrheim, Nuovo Cimento B **37**, 1 (1977).

[14] A. Stern, Nature **464**, 187 (2010).

[15] K. Shtengel, Physics **3**, 93 (2010).

[16] F.D.M. Haldane, Phys. Rev. Lett. **55**, 20 (1985).

[17] D. Yoshioka, B.I. Halperin and P.A. Lee, Phys. Rev. Lett. **50**, 1219 (1983).

[18] R. Tao, and D.J. Thouless, Phys. Rev. B **28**, 1142 (1983).

[19] P.W. Anderson, Phys. Rev. B **28**, 2264 (1983).

[20] W.P. Su, Phys. Rev. B **30**, 1069 (1984).

[21] W.P. Su and J.R. Schrieffer, Phys. Rev. Lett. **46**, 738 (1981).

[22] E.J. Bergholtz, and A. Karlhede, J. Stat. Mech. (2006) L04001.

[23] E.J. Bergholtz, T. H. Hansson, M. Hermanns, and A. Karlhede, Phys. Rev. Lett. **99**, 256803 (2007).

[24] E.J. Bergholtz, and A. Karlhede, Phys. Rev. B **77**, 155308 (2008).

[25] E.J. Bergholtz, and A. Karlhede, Phys. Rev. Lett. **94**, 26802 (2005).

[26] E.H. Rezayi and F.D.M. Haldane, Phys. Rev. B **50**, 17199 (1994).

[27] A. Seidel, H. Fu, D.-H. Lee, J.M. Leinaas and J. Moore, Phys. Rev. Lett. **95**, 266405 (2005).

[28] G. Moore and N. Read, Nucl. Phys. B **360**, 362 (1991).

[29] M. Greiter, X.-G. Wen and F. Wilczek, Phys. Rev. Lett. **66**, 3205 (1991); Nucl. Phys. **B374**, 567 (1992).

[30] E.H. Rezayi and F.D.M. Haldane, Phys. Rev. Lett. **84**, 20 (2000).

[31] F.D.M. Haldane in *The Quantum Hall Effect*, eds. R.E. Prange and S.M. Girvin, (Springer-Verlag, New York, 1990).

[32] N.K. Wilkin, J.M.F. Gunn, and R.A. Smith, Phys. Rev. Lett. **80**, 2265 (1998).

[33] N.R. Cooper and N.K. Wilkin, Phys Rev. B **60**, 16279(R) (1999).

[34] S. Viefers, J. Phys.: Condens. Matter **20** 123202 (2008).

[35] N.R. Cooper, N.K. Wilkin, and J.M.F. Gunn, Phys. Rev. Lett. **87**, 120405 (2001).

[36] N. Regnault and Th. Jolicoeur, Phys. Rev. Lett. **91**, 030402 (2003); Phys. Rev. B **69**, 235309 (2004); Phys. Rev. B **76**, 235324 (2007).

[37] C.C. Chang, N. Regnault, Th. Jolicoeur, and J.K. Jain, Phys. Rev. A **72**, 013611 (2005); N. Regnault, C.C. Chang, Th. Jolicoeur, and J.K. Jain, J. Phys. B **39**, 89 (2006).

[38] E. Wikberg, *Non-abelian Quantum Hall states on the Thin Torus*, Licentiate thesis (2009).

[39] N. Read, and E.H. Rezayi, Phys. Rev. B **54**, 16864 (1996).

[40] O. Bratteli, Trans. Amer. Math. Soc. **171**, 195 (1972).

[41] J. Hubbard, Phys. Rev. B **17**, 494 (1978).

[42] I. Bloch, J. Dalibard, and W. Zwerger, Rev. Mod. Phys. **80**, 885 (2008).

[43] M. Lewenstein, A. Sanpera, V. Ahufinger, B. Damski, A. Sen(De), and U. Sen, Adv. Phys. **56**, 243 (2007).

[44] D.B.M. Dinkerscheid, U. Al Khawaja, D. van Oosten, and H.T.C. Stoof, Phys. Rev. A **71**, 043604 (2005).

[45] For a review on the extensive work done in this area, see T. Lahaye, C. Minotti, L. Santos, M. Lewenstein, and T. Pfau, Rep. Prog. Phys. **72**, 126401 (2009).

[46] V.L. Pokrovsky, and G.V. Uimin, J. Phys. C: Solid State Phys. **11**, 3535 (1978).

[47] F.J. Burnell, M.M. Parish, N.R. Cooper, and S.L. Sondhi, Phys. Rev. B **80**, 174519 (2009).

[48] M. Bauer, and M.M. Parish, Phys. Rev. Lett. **108**, 255302 (2012).

[49] M. Iskin, Phys. Rev. A **83**, 051606 (2011).

[50] D.L. Kovrizhin, G. Venketeswara Pai, and S. Sinha, Europhys. Lett. **72** 162 (2005).

[51] A. Griesmaier, J. Werner, S. Hensler, J. Stuhler, and T. Pfau, Phys. Rev. Lett. **94**, 160401 (2005); K.K. Ni, S. Ospelkaus, M.H.G. de Miranda, A. Peer, B. Neyenhuis, J.J. Zirbel, S. Kotochigova, P.S. Julienne, D.S. Jin, and J. Ye, Science **322**, 231 (2008); J.G. Danzl, M.J. Mark, E. Haller, M. Gustavsson, R. Hart, J. Aldegunde, J.M. Hutson, and H.-C. Nägerl, Nature Phys. **6**, 265 (2010).

[52] For different methods for varying μ locally, see, e.g., C. Weitenberg, M. Endres, J.F. Sherson, M. Cheneau, P. Schauss, T. Fukuhara, I. Bloch, and S. Kuhr, Nature **471**, 319 (2011); U. Gavish and Y. Castin, Phys. Rev. Lett. **95**, 020401 (2005).

[53] M. Kardell, and A. Karlhede, J. Stat. Mech., P02037 (2011).

Part II:
Accompanying papers